Author/s:
Brydon, SC;Thomson, C;O'Hair, RAJ;White, JM

Title:
Electronic and Steric Effects on the Reactivity of Seleniranium Ions with Alkenes in the Gas Phase

Date:
2023-07-21

Citation:
Brydon, S. C., Thomson, C., O'Hair, R. A. J. & White, J. M. (2023). Electronic and Steric Effects on the Reactivity of Seleniranium Ions with Alkenes in the Gas Phase. Journal of Organic Chemistry, 88 (14), pp.9629-9644. https://doi.org/10.1021/acs.joc.2c02233.

Persistent Link:
https://hdl.handle.net/11343/332887

The Journal of Organic Chemistry

Steric and Electronic Effects on the Reactivity of Seleniranium Ions with Alkenes in the Gas Phase

Samuel C. Brydon,*[,a] Catriona Thomson,[a] Richard A. J. O'Hair,[a] Jonathan M. White.*[,a]

[a]School of Chemistry and Bio21 Institute, The University of Melbourne, Parkville, VIC 3010, Australia

ABSTRACT

Gas phase ion-molecule reactions between seleniranium ions, R-*c*-$SeCH_2CH_2^+$, and *cis*-cyclooctene were used to probe steric and electronic effects of substituents on kinetics and branching ratios. The second order rates increased in the order: *p*-$OMeC_6H_4$ < C_6H_5 < *p*-BrC_6H_4 < *p*-$CF_3C_6H_4$ < *m*-$NO_2C_6H_4$ giving a Hammett plot with $R^2 = 0.98$ and $\rho = +1.66$. The two main pathways include direct transfer of the selenium moiety to the incoming alkene (π-ligand exchange) and the less favoured ring-opening by attack at an iranium carbon giving a *cis*-bicyclic selenonium ion as supported by density functional theory (DFT) calculations. Branching ratios of each pathway indicated that electron withdrawing groups directed more attack at carbon than the selenium in agreement with previous solution phase results. Increased steric bulk on the selenium was investigated by changing the R group from a methyl to *t*-butyl, which not only shut down π-ligand exchange, but also significantly reduced overall reactivity. Finally, the reactivity of the iranium ion derived from *Se*-methylselenocysteine was investigated and shown to react faster and favour π-ligand exchange as the leaving group was changed from ethene to acrylic acid.

INTRODUCTION

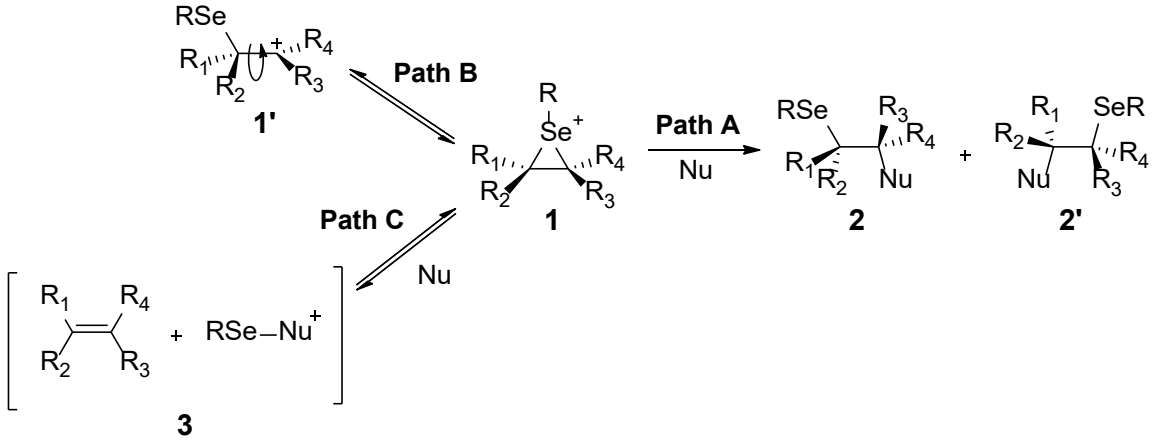

Scheme 1. Potential reaction pathways of enantioenriched seleniranium ion **1** (**A**) nucleophilic attack at carbon to afford addition products **2** or **2'** with retention of stereochemistry, (**B**) racemisation *via* bond rotation, or (**C**) nucleophilic attack at selenium leading to racemisation.

Seleniranium ions have the general structure **1** and can be formed through the displacement of a suitable β-leaving group or by the addition of a selenium electrophile to a carbon-carbon double bond.[1, 2] When enantioenriched, ring opening of these intermediates by nucleophiles in principle affords products **2** or **2'** with retention of stereochemical integrity, noting that intramolecular nucleophiles furnish cyclised products (**Path A**, **Scheme 1**). This pathway has been exploited by many groups to functionalise alkenes

with the aim to develop methods that are both enantioselective and catalytic as highlighted in several recent reviews,[3-7] where Denmark and co-workers have established Lewis base activation of the intermediate seleniranium ion as a particularly useful approach for several transformations.[8-10] However, there are two plausible racemisation pathways available to chalcogen iranium ions that must be controlled to minimise loss of enantiopurity.[9, 11] The first is ring opening to give a carbocation **1'** followed by bond rotation, which can be minimised by judicious choice of the substituents on the ring carbons (**Path B**, **Scheme 1**). The second is preventing nucleophilic attack at the electrophilic selenium, which is more challenging as illustrated by numerous reports in the literature of configurational scrambling by deselenylation from either inter- (including counterions or solvent) or intramolecular (e.g. pendant alcohols or carboxylic acids) nucleophiles generating the electrophilic reagent **3**, which can be recaptured by the alkene leading to racemisation of the initial seleniranium ion **1** (**Path C**, **Scheme 1**).[9, 12-15]

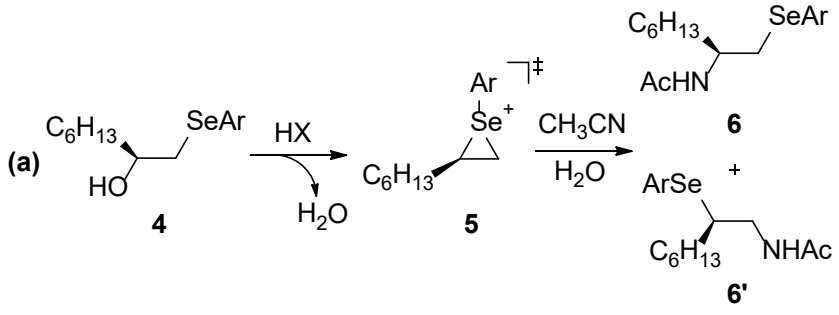

Aryl group	es, %
C_6H_5	13
2,6-$(CH_3)_2C_6H_3$	30
2,4,6-(*i*-Pr)$_3C_6H_2$	35
2,4,6-(*t*-Bu)$_3C_6H_2$	100
4-$CF_3C_6H_4$	70
2-$CF_3C_6H_4$	98
2,6-$(CF_3)_2C_6H_3$	99

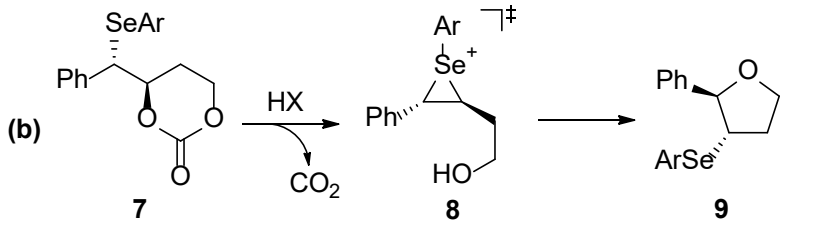

Aryl group	es, %
4-$OMeC_6H_4$	5
C_6H_5	17
2,4,6-(*i*-Pr)$_3C_6H_2$	30
4-$CF_3C_6H_4$	27
2-$CF_3C_6H_4$	40
2-$NO_2C_6H_4$	>99
2,6-$(CF_3)_2C_6H_3$	>99

Scheme 2. Effect of varying the arylseleno group on enantiospecificity (es, %) in (**a**) seleno-Ritter reaction proceeding *via* intermolecular capture of seleniranium ion **5** (ratio of products **6**:**6'** approximately 9:1),[16] and (**b**) acid mediated carbonate ring-opening of **7** proceeding *via* intramolecular capture of seleniranium ion **8**.[9] The discrepancies between the two studies for the enantiospecificity outcomes of the 2- and 4-trifluoromethylphenyl substituents may plausibly be due to the intramolecular nature of the nucleophile in (**b**) allowing for more competitive deselenylation.

The most effective methods developed to suppress this pathway involve blocking nucleophiles from directly attacking at the selenium. The use of steric bulk has been employed by Toshimitsu and co-workers in a seleno-Ritter reaction, where increasing the size of the substituents on the aryl ring *ortho* to the selenium led to complete retention of stereochemical purity (**a**, **Scheme 2**).[15-17] Electron withdrawing groups such as the 4-trifluoromethylphenyl substituent also decreased racemisation with an optical yield of 70% obtained compared to 13% for the unsubstituted phenyl group.[16] A similar strategy was used by Denmark and co-workers for carbonate ring-opening reactions with a 2,6-bis(trifluoromethyl)phenyl on the selenium resulting in >99% es due to a combination of steric bulk disfavouring attack at the selenium and the electron withdrawing nature of the substituents activating the endocyclic carbons of the seleniranium ion towards nucleophilic attack (**b**, **Scheme 2**).[9] In the latter study, retention of enantiopurity was obtained with the more strongly electron withdrawing 2-nitrophenyl substituent, where an additional through-space n_O-$\sigma^*_{Se\text{-}C}$ interaction was postulated to explain the >99% es stereochemical outcome. This chalcogen bonding interaction has been invoked to rationalise the outcomes in a number of enantioselective reactions proceeding *via* seleniranium ions and observed in crystal structures of *ortho*-substituted phenylselenyl species.[14, 18, 19] Toshimitsu also found

that a 2-pyridyl substituent gave excellent enantiopurity in a variety of reactions,[20, 21] but reactions of 2-pyridylselenyl halides with alkenes by Potapov *et al.* suggest substantial involvement of a five-membered cyclic pyridinium ion.[22]

Outside of the effects of *ortho* substituents on the racemisation of seleniranium ions, little attention has been paid to electronic effects of *meta* or *para* substituents on their configurational stability. Denmark found that the electron donating 4-methoxyphenyl reduced the es to 5% compared to the unsubstituted phenyl 17%, which was lower than the 27% attained using the electron withdrawing 4-trifluoromethylphenyl group (**b**, **Scheme 2**).[9] Though this ordering is explained by the above rationale of the increase in electrophilicity of the iranium ion endocyclic carbons, the potential for product racemisation was not tested for the 4-methoxyphenyl substituent. Given the potential for ring opening to be enhanced by more electron-rich selenium substituents, particularly in the presence of acid, the 5% es obtained is not necessarily due to greater racemisation at the initial seleniranium ion. Thus, one question posed here is whether making the selenium more electron rich would lead to more attack at the heteroatom or attack at one of the iranium carbons. This is particularly informative if the selenium cation transfer is desirable as studies by Bock and co-workers have utilised this transfer from seleniranium ions to alkenes to initiate polyene cyclisations.[23, 24]

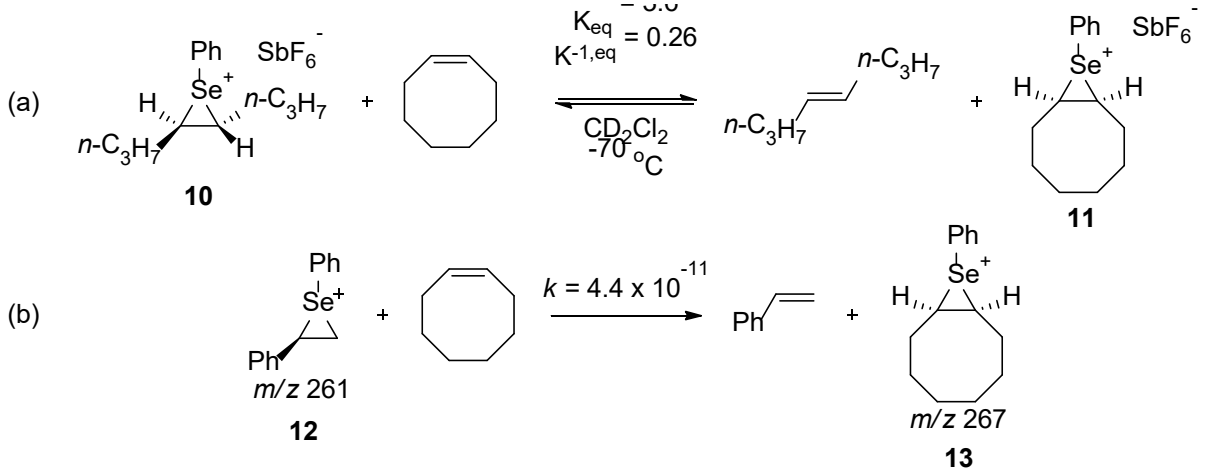

Scheme 3. Observations of π-ligand exchange in **(a)** solution phase NMR by reacting seleniranium ions **10** with alkenes at -70 °C in the presence of a hexafluoroantimonate counterion and measured equilibrium constants,[2, 9] and **(b)** gas phase ion-molecule reactions between seleniranium ions **12** and alkenes and experimental second order rate coefficient (in units of cm^3 $molecule^{-1}$ s^{-1}).[25]

The process of an alkene nucleophile attacking the electrophilic selenium is known as associative π-ligand exchange since another seleniranium ion is generated (Nu = alkene in **Path C**, **Scheme 1**). This process is particularly rapid for selenium with observations of direct transfer of the selenium moiety at -70 °C in solution (**a**, **Scheme 3**) and is a significant racemisation pathway during alkene functionalisation.[2, 9] Even when the 2-nitrophenyl group is employed, a loss of enantiospecificity (88% *vs* > 99%) was observed in the carbonate ring opening experiments when an equivalent of *trans*-4-phenyl-3-buten-1-ol was present in the reaction mixture, with the erosion attributed to the alkene rather than the alcohol from control experiments. To avoid the complications of solvent, counterions or additives facilitating this transfer *via* a dissociative mechanism, gas phase studies of chalcogen iranium ions such as **12**, generated from appropriate precursors under electrospray ionisation (ESI) conditions, reacting with alkenes in a linear ion trap mass spectrometer have provided fundamental insights into kinetics and branching ratios (**b**, **Scheme 3**).[25-27] This work extends these studies to examine electronic effects upon the reactivity of seleniranium ions with alkenes in the gas phase and to determine whether the same trends observed in solution phase translate into the gas phase.

RESULTS AND DISCUSSION

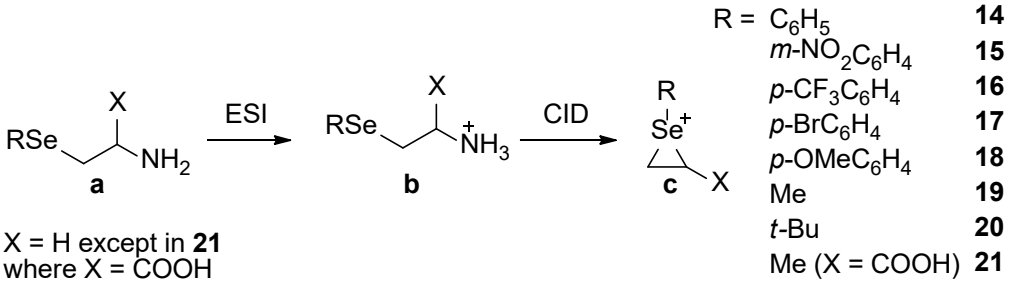

Scheme 4. Generation of seleniranium ions **14c-21c** *via* electrospray ionisation (ESI) of the β-selenoethylamines with subsequent collision-induced dissociation (CID) of the protonated ammonium ion **14b-21b**. Note that **21a** was introduced as the hydrochloride salt.

Substituted 2-selenoethylamines **14a-20a** or hydrochloride salt **21a** were introduced into the ion trap mass spectrometer *via* the electrospray ionisation (ESI) source as *ca* 0.1 mM solutions in methanol (**14a-20a**) or 50:50 methanol/water (**21a**) (**Scheme 4**, see Experimental Section for further detail). The ammonium ions **14b-21b** were mass-selected and fragmented to give **14c-21c** *via* CID using a normalised collision energy (NCE) of 15% in a MS^2 experiment. The seleniranium ions **14c-21c** were the major product ion in most cases, but other species were competitive such as the stabilised *p*-$OMeC_6H_4Se^+$ ion from CID of ammonium ion **18b** (see **Figures S15** and **S16** in the SI). The seleniranium ions **14c-21c** were then further mass selected in a MS^3 experiment for ion-molecule reactions (IMR).

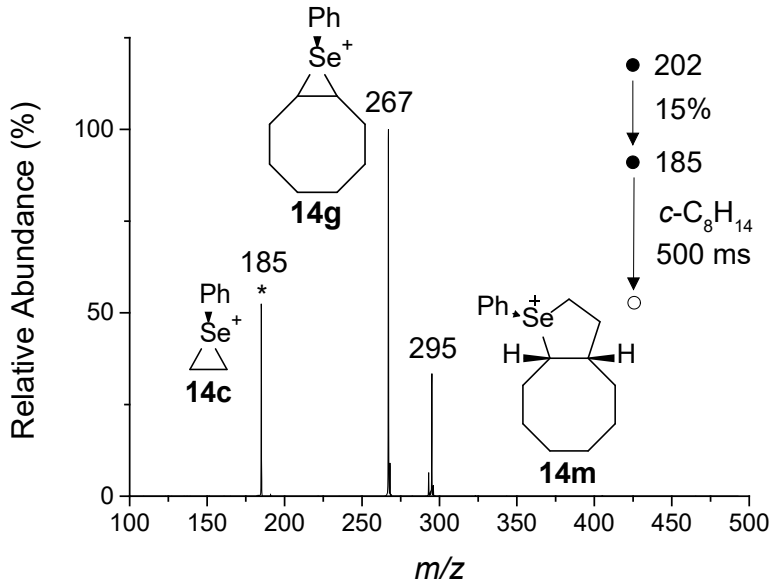

Figure 1. MS^3 IMR of *cis*-cyclooctene with ethyl phenylseleniranium ion **14c** (*m/z* 185, *) to give *cis*-cyclooctyl phenylseleniranium **14g** (*m/z* 267) *via* π-ligand exchange and *cis*-bicyclic selenonium ion **14m** (*m/z* 295) *via* addition at t = 500 ms. [*cis*-cyclooctene] = 5.3 × 10^{11} molecule cm^{-3}. The most abundant ^{80}Se isotope of **14c** was mass-selected following CID (NCE of 15%) of ammonium ion **14b** (*m/z* 202). See **Figure S17D** in the SI for HRMS.

Initially, the phenylseleniranium ion **14c** (*m/z* 185) was mass selected in a MS^3 experiment and allowed to undergo reaction with neutral *cis*-cyclooctene introduced into the ion trap *via* the helium bath gas line. This alkene was chosen as it has been shown to be one of the most reactive neutrals, due to the

release of ring strain during the reaction, making it suitable for our experimental set up.[25, 26] The resulting spectrum at a reaction time of 500 ms is shown in **Figure 1** and displays two new peaks at *m/z* 267 and *m/z* 295. The former corresponds to the π-ligand exchange product **14g**, where *cis*-cyclooctene has displaced ethene at the electrophilic selenium atom (**Scheme 5A**). Alternatively, the alkene may attack at one of the iranium carbons to ring open the strained three-membered ring. Subsequent intramolecular capture of the intermediate carbocation by the selenium furnishes the *cis*-bicyclic selenonium ion **14m** observed at *m/z* 295 (**Scheme 5B**).

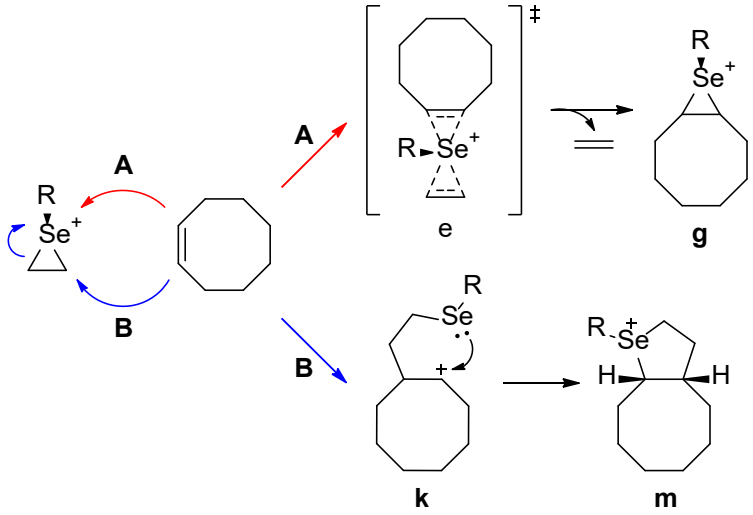

Scheme 5. Mechanism for (**A**) π-ligand exchange involving transfer of the electrophilic selenium atom from ethene in **c** to *cis*-cyclooctene in **g** proceeding *via* a Hückel pseudocoarctate transition state **e**,[28, 29] and (**B**) formation of the *cis*-bicyclic addition product **m** by initial ring opening of the seleniranium ion **c** by *cis*-cyclooctene with subsequent capture of the secondary carbocation intermediate **k**.[26, 30]

To investigate substituent electronic effects on both the reaction rate and the reaction partitioning of the seleniranium ion with *cis*-cyclooctene, substituents at the *meta* and *para* positions of the Se-phenyl ring were introduced (avoiding the complications of the *ortho* substituents as mentioned). These covered a range of electron withdrawing substituents as indicated by the Hammett σ constant from *m*-nitro (σ = 0.710) > *p*-trifluoromethyl (σ = 0.54) > *p*-bromo (σ = 0.232) to the electron donating *p*-methoxy (σ = -0.268).[31] In the same fashion as the unsubstituted phenyl system **14c** (*m/z* 185), the seleniranium ions **15c** (*m*-NO_2, *m/z* 230), **16c** (*p*-CF_3, *m/z* 253), **17c** (*p*-Br, *m/z* 263), and **18c** (*p*-OMe, *m/z* 215) were isolated in a MS^3 experiment and allowed to react with *cis*-cyclooctene. The same two reaction channels were observed for all ions with both π-ligand exchange (*m*-NO_2: *m/z* 312, *p*-CF_3: *m/z* 335, *p*-Br: *m/z* 345, *p*-OMe: *m/z* 297) and addition (*m*-NO_2: *m/z* 340, *p*-CF_3: *m/z* 363, *p*-Br: *m/z* 373, *p*-OMe: *m/z* 325) observed as the major product ions (**Figure 2**). From examination of the spectra recorded at the reaction time when the precursor ion relative abundance was approximately 50%, it was evident that the kinetics and reaction partitioning differ greatly depending on the electronic nature of the aryl substituent on the selenium with the more electrophilic ions reacting faster and giving more addition product relative to π-ligand exchange.

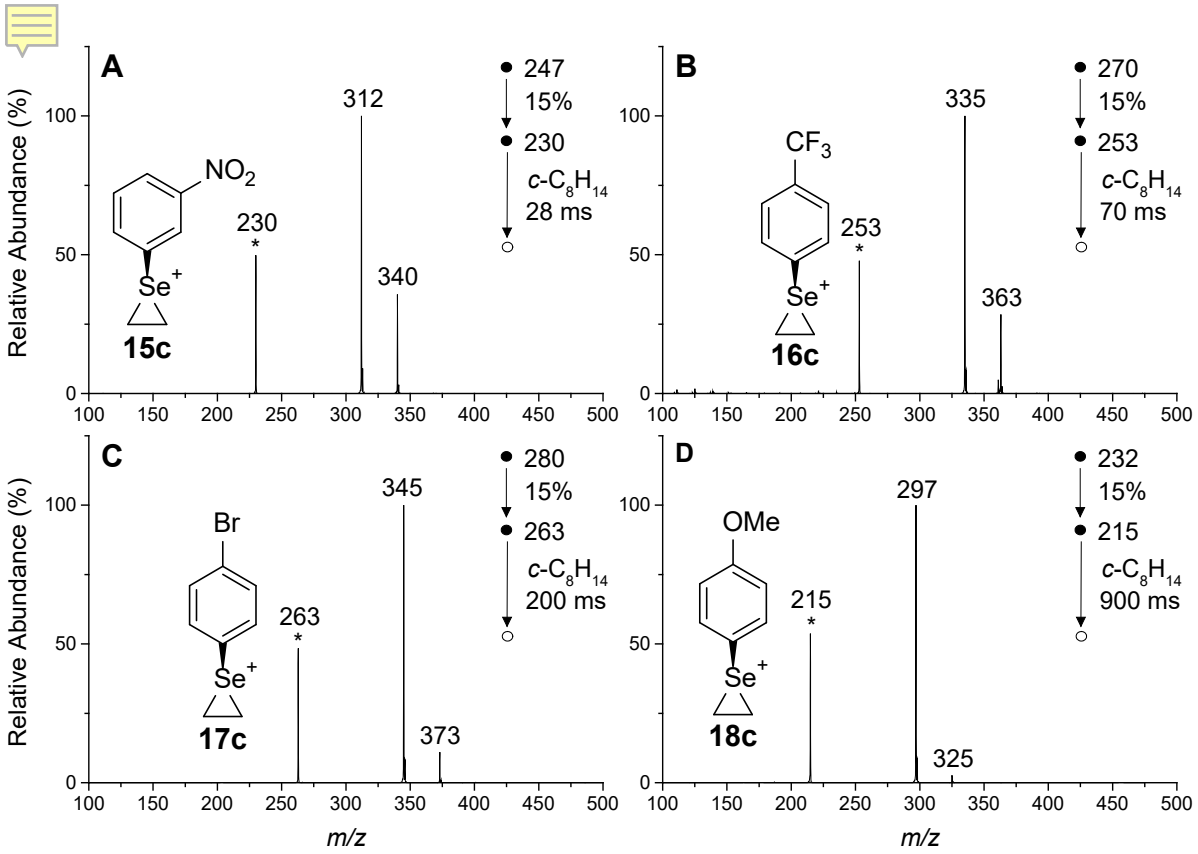

Figure 2. MS^3 IMR of *cis*-cyclooctene with (**A**) *m*-nitrophenylseleniranium ion **15c** (*m/z* 230, *) to give products **15g** (*m/z* 312) and **15m** (*m/z* 340) at t = 28 ms, (**B**) *p*-trifluoromethylphenylseleniranium ion **16c** (*m/z* 253, *) to give products **16g** (*m/z* 335) and **16m** (*m/z* 363) at t = 70 ms, (**C**) *p*-bromophenylseleniranium ion **17c** (*m/z* 263, *) to give products **17g** (*m/z* 345) and **17m** (*m/z* 373) at t = 200 ms, and (**D**) *p*-methoxyphenylseleniranium ion **18c** (*m/z* 215, *) to give products **18g** (*m/z* 297) and **18m** (*m/z* 325) at t = 900 ms. [*cis*-cyclooctene] = 5.3×10^{11} molecule cm^{-3}. The most abundant ^{80}Se isotope of **15c-18c** was mass-selected (*) following CID (NCE of 15%) of ammonium ions **15b-18b**, though for *p*-bromoseleniranium **17c** there is a mixture of $^{78}Se/^{81}Br$ and $^{80}Se/^{79}Br$ isotopes. See **Figures S17A-C** and **E** in the SI for HRMS.

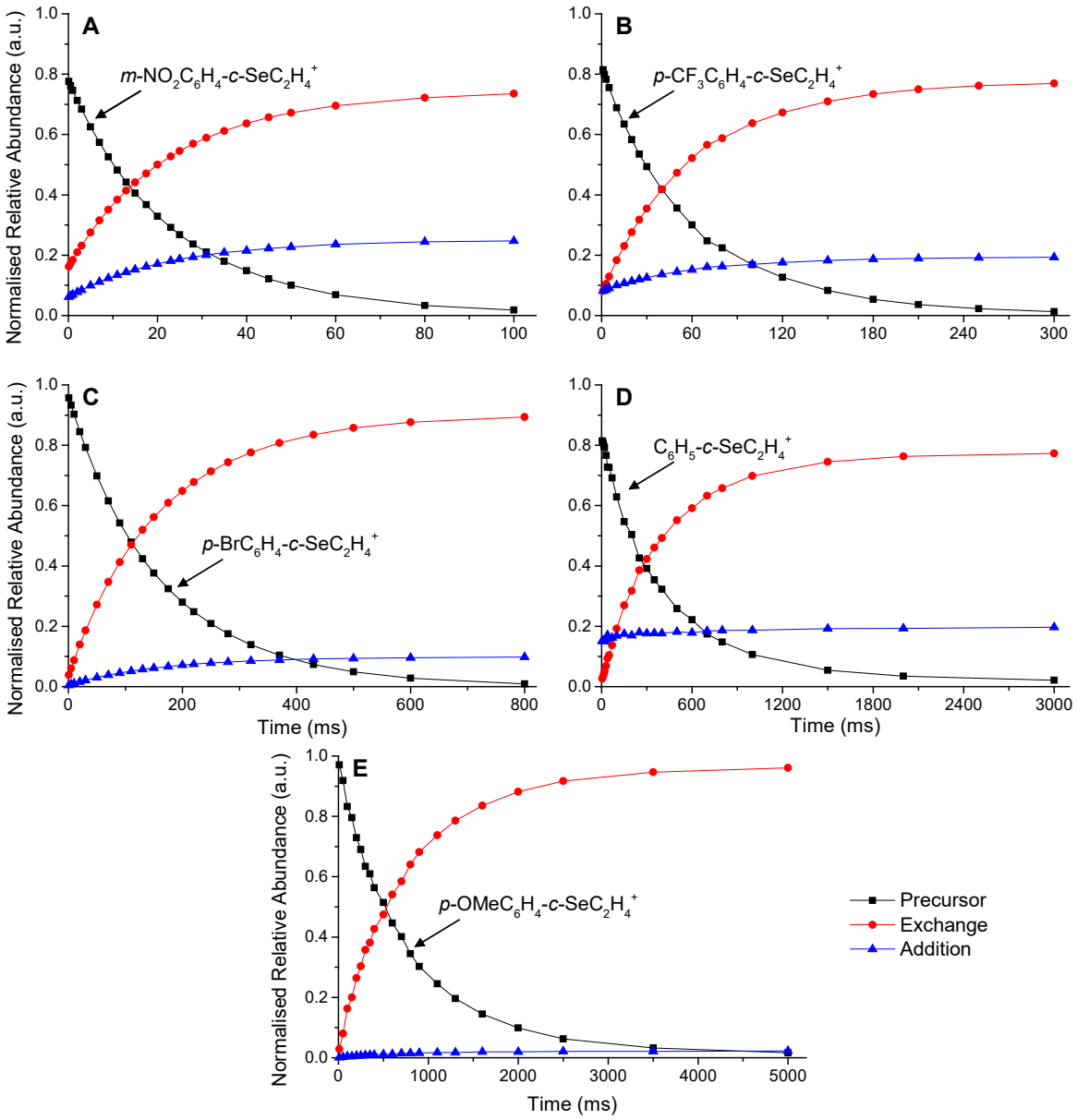

Figure 3. Kinetic curves for MS^3 IMR of *cis*-cyclooctene (5.3×10^{11} molecule cm^{-3}) with (**A**) *m*-nitrophenylseleniranium ion **15c** (*m/z* 230, black squares) to give products **15g** (*m/z* 312, red circles) and **15m** (*m/z* 340, blue triangles), (**B**) *p*-trifluoromethylphenylseleniranium ion **16c** (*m/z* 253, black squares) to give products **16g** (*m/z* 335, red circles) and **16m** (*m/z* 363, blue triangles), (**C**) *p*-bromophenylseleniranium ion **17c** (*m/z* 263, black squares) to give products **17g** (*m/z* 345, red circles) and **17m** (*m/z* 373, blue triangles), (**D**) phenylseleniranium ion **14c** (*m/z* 185, black squares) to give products **18g** (*m/z* 267, red circles) and **18m** (*m/z* 295, blue triangles), and (**E**) *p*-methoxyphenylseleniranium ion **18c** (*m/z* 215, black squares) to give products **18g** (*m/z* 297, red circles) and **18m** (*m/z* 325, blue triangles). Each point represented the intensity of the ion peak(s) as a proportion of the total ion intensity at various reaction times (ms), noting that isotope peaks of the product ions have been summed together. Kinetic curves for early onset of reaction of (**A**), (**B**) and (**D**) measured at a lower concentration of *cis*-cyclooctene (5.3×10^{10} molecule cm^{-3}) are provided in **Figure 7** for (**D**) and **Figure S18** for (**A**) and (**B**) in the SI.

To understand the kinetics of these reactions, the relative abundancies of the precursor and product ions were plotted as a function of reaction time (**Figure 3**). In all cases at longer reaction times, the π-ligand

exchange product (red circles) dominates as the preferred pathway to addition (blue triangles) as reflected in the mass spectra (**Figure 1** and **Figure 2**). However, the early onset of the reaction appears more complicated, particularly when comparing the reactivity of the unsubstituted phenylseleniranium **14c** with the more electron deficient *p*-bromophenyl **17c** and more electron rich *p*-methoxyphenyl **18c**. There appears to be rapid growth of the addition product **14m** initially and to a lesser extent for the formation of **16m**. Given that the π-ligand exchange pathway is exclusive to the three-membered ring and is hence diagnostic of the seleniranium ion structure, this suggests the presence of a more reactive isomer at early time points. This shall be further explored later, but analysis of the iranium ion kinetics was carried about by excluding the initial consumption of the precursor ion to titrate out the isomeric impurity.[32, 33]

Table 1. Experimental second order rate coefficients (k_2), theoretical collision rate coefficients from average dipole orientation theory (k_{ADO}) and reaction efficiency (φ) for ion-molecule reactions of aryl substituted seleniranium ions **14c-18c** with *cis*-cyclooctene

No.	Aryl	*m/z*	k_2 ($\times 10^{-11}$)[a,b]	k_{ADO} ($\times 10^{-9}$)[a]	φ (%)[c]	σ^{31}
15c	*m*-$NO_2C_6H_4$	230	7.35 ± 0.26	1.04	7.1	0.710
16c	*p*-$CF_3C_6H_4$	253	2.74 ± 0.06	1.02	2.7	0.54
17c	*p*-BrC_6H_4	263	1.11 ± 0.05	1.02	1.1	0.232
14c	C_6H_5	185	0.31 ± 0.03	1.08	0.3	0
18c	*p*-$OMeC_6H_4$	215	0.18 ± 0.02	1.05	0.2	-0.268

[a] Units of rate coefficients are cm^3 $molecule^{-1}$ s^{-1}. [b] Errors are given as one standard deviation from at least five independent measurements, though a conservative error is ± 25%.[34] [c] $\varphi = (k_2/k_{ADO}) \times 100$ %

To quantify the reactivity between the various phenylseleniranium ions **14c-18c**, Ar-*c*-$SeCH_2CH_2^+$, and *cis*-cyclooctene, *pseudo* first order rate coefficients were initially obtained from the kinetic curves (see Experimental Section and SI **Figure S19**). The subsequently derived second order rate coefficients for consumption of the precursor ion (in units of cm^3 $molecule^{-1}$ s^{-1}) increase in the order *p*-$OMeC_6H_4$ **18c** ($k_2 = 0.18 \times 10^{-11}$) < C_6H_5 **14c** ($k_2 = 0.31 \times 10^{-11}$) < *p*-$BrC_6H_4$ **17c** ($k_2 = 1.11 \times 10^{-11}$) < *p*-$CF_3C_6H_4$ **16c** ($k_2 = 2.74 \times 10^{-11}$) < *m*-$NO_2C_6H_4$ **15c** ($k_2 = 7.35 \times 10^{-11}$) as expected based on the Hammett σ constants, giving over a 40-fold increase in rate from the least to most reactive species (**Table 1**). The collision rate coefficient k_{ADO} was calculated from average dipole orientation (ADO) theory and slightly increases as the ion becomes lighter since the other determining factors are the neutral characteristics, which are the same for all reactions. Since k_{ADO} is approximately 1×10^9 cm^3 $molecule^{-1}$ s^{-1}, the reaction efficiency φ increases as the second order rate coefficient increases from 0.2% (aryl = *p*-$OMeC_6H_4$) to 7.1% (aryl = *m*-$NO_2C_6H_4$). The reactions are all relatively inefficient, indicating that rather than forming product ions a large proportion of the reactant ions form the initial ion-molecule complex for one of the two channels, but dissociate to the separated reactants at some point along the reaction coordinate. This reflects the competition between the rate of back dissociation, which has a very "loose" transition state, and the more ordered, "tighter" transition states of the product channels. [35, 36]

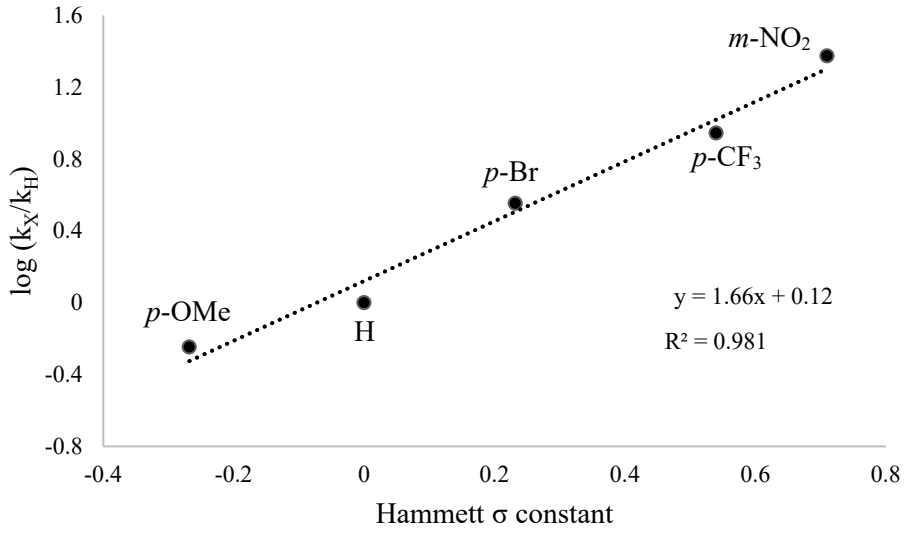

Figure 4. Hammett plot of the relative rate coefficients from reaction of *cis*-cyclooctene with seleniranium ions **14c-18c**. ρ = +1.66, R^2 = 0.98.

A Hammett plot of the logarithm of the relative reaction rate for each substituted phenyl system **15c-18c** compared to the unsubstituted system **14c**, log(k_X/k_H), against the σ constant gives a good linear correlation with R^2 = 0.98 (**Figure 4**).[26, 37-40] The positive slope with ρ = + 1.66 reflects the increasing reaction rate as the seleniranium ion becomes more reactive as the phenyl group becomes more electron deficient. This may be rationalised by both the selenium and iranium carbon atoms becoming more electrophilic, the latter becoming activated since the selenium-carbon bond of the three-membered ring is weakened as electron density of the selenium is more effectively delocalised into the phenyl ring (*vide supra*).[9] The positive ρ value suggests that both the π-ligand exchange and addition pathways are likely responding in a similar way to the electronic nature of the substituents, but it is not clear from this plot to what extent each pathway is affected. The reaction constant determined in this study is very similar to that determined previously for varying electron demand at the iranium carbon for addition of *cis*-cyclooctene to styryl derived thiiranium ions (ρ = + 1.69),[26] suggesting that changing the electron demand at any atom of the three-membered ring will affect the overall change in reactivity of a chalcogen iranium ion in a similar way.

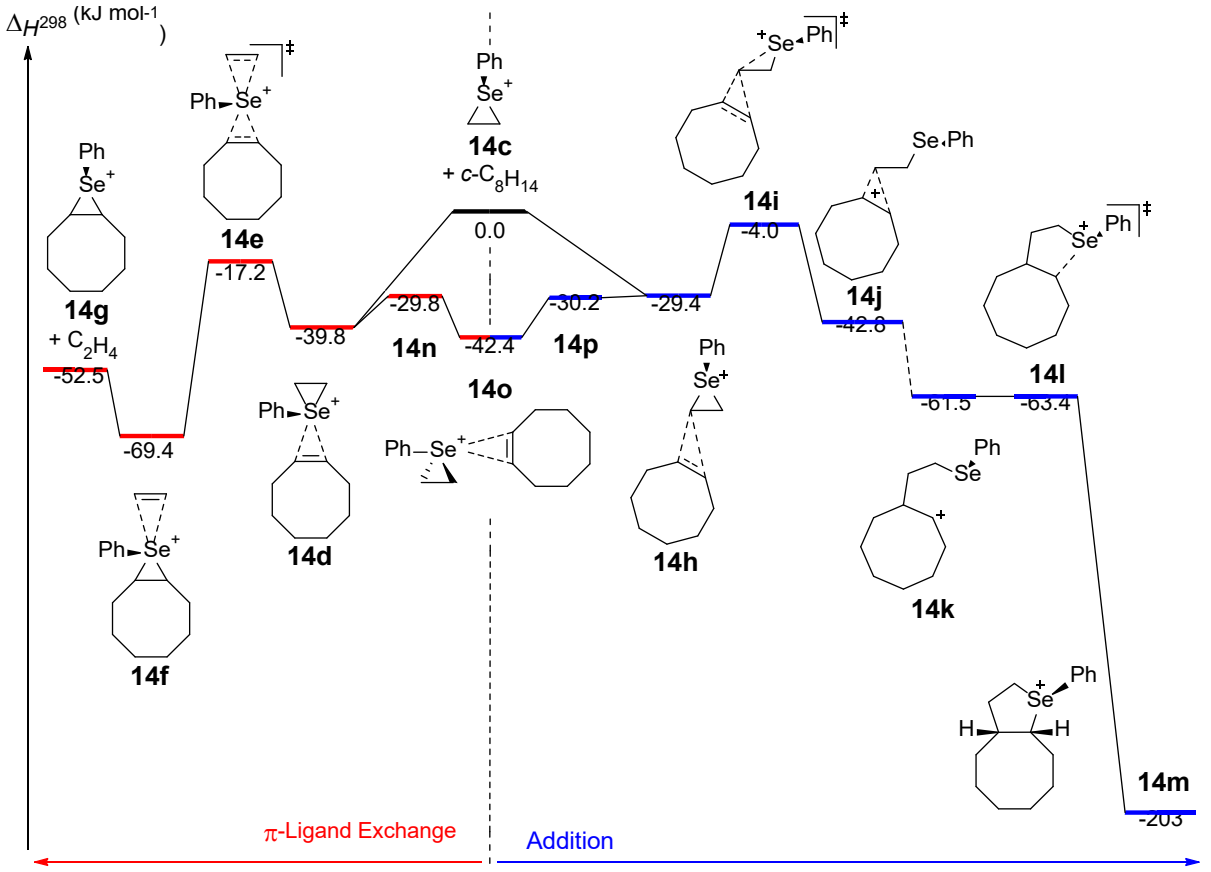

Figure 5. Relative enthalpy diagram for ion-molecule reaction of phenylseleniranium ion **14c** (*m/z* 185) with *cis*-cyclooctene proceeding *via* π-ligand exchange (red) to give **14g** (*m/z* 267) or addition (blue) to give **14m** (*m/z* 295). Enthalpies (ΔH) in kJ mol^{-1} at 298 K are calculated at M06-2X-D3/def2-TZVP.

To explore how changing the electronic nature of the aryl substituent on the selenium atom affects the overall reactivity, DFT calculations were performed to map out the relative energy diagrams of the two reaction channels. The relative enthalpies for the competing π-ligand exchange and addition pathways for the reaction of the unsubstituted phenylseleniranium ion **14c** (*m/z* 185) with *cis*-cyclooctene are provided in **Figure 5**. The former involves the barrierless formation of an initial ion-molecule association complex **14d**, where the incoming alkene coordinates to the selenium atom (ΔH_d = - 39.8 kJ mol^{-1}). The rate determining step for this pathway is then the transfer of the selenium moiety between alkenes *via* a Hückel pseudocoarctate transition state **14e** -17.2 kJ mol^{-1} below the reactants ($\Delta H^{\ddagger}_e$), or +22.6 kJ mol^{-1} above the preceding complex ($\Delta\Delta H^{\ddagger}_\pi$). Following this exothermic isomerisation to the dissociation complex **14f** (ΔH_f = - 69.4 kJ mol^{-1}), where the departing ethene is now weakly bound, the observed *cis*-cyclooctyl seleniranium ion **14g** (*m/z* 267) is produced following the loss of ethene. The reaction is overall exothermic, ΔH_g = -52.5 kJ mol^{-1}, with the difference in energy largely due to the significant ring strain release from *cis*-cyclooctene.[25, 26]

The addition channel involves initial formation of an alternative ion-molecule complex **14h** between *cis*-cyclooctene and one of the iranium carbons (ΔH_h = - 29.4 kJ mol^{-1}). The seleniranium ion is then spontaneously ring opened given the exothermic barrier **14i** ($\Delta H^{\ddagger}_i$ = - 4.0 kJ mol^{-1}) leading to an intermediate carbocation **14j** (ΔH_j = - 42.8 kJ mol^{-1}).[26] Bond rotation (not shown) gives a discrete secondary carbocation **14k** (ΔH_k = - 61.5 kJ mol^{-1}), which readily closes *via* transition state **14l** ($\Delta H^{\ddagger}_l$ = - 63.4 kJ mol^{-1}) to give the *cis*-bicyclic product **14m** with an overall exothermicity of -203 kJ mol^{-1}. The kinetically favourable π-ligand exchange pathway ($\Delta H^{\ddagger}_e$ = -17.2 kJ mol^{-1}) will thus outcompete the addition pathway ($\Delta H^{\ddagger}_i$ = - 4.0 kJ mol^{-1}), which is reflected in the mass spectrum for the iranium ion **14c** IMR (**Figure 1**). The partitioning is also dependent on other factors such as the relative enthalpies

of the initial ion-molecule complexes **14d** and **14h**,[34] with interconversion potentially proceeding *via* a chalcogen-bonded complex **14o**, where the *cis*-cyclooctene interacts with the $\sigma^*_{Se\text{-}CAr}$ antibonding orbital. However, given that π-ligand exchange has the lower energy initial complex (ΔH_d = - 39.8 kJ mol^{-1}) than addition (ΔH_h = - 29.4 kJ mol^{-1}) and is irreversible after the ethene is lost (neutrals are removed by the vacuum), whilst the addition pathway is reversible as the ions are still "hot" prior to collisional cooling with helium bath gas,[41] any interconversion would still favour the transfer of the selenium moiety to the cycloalkene.

Comparison to the addition of *cis*-cyclooctene to the thiiranium ion congener (*m/z* 137) studied previously shows a much faster rate of reactivity for selenium *vs* sulfur ($k_2 = 31 \times 10^{-13}$ *vs* 0.37×10^{-13} cm^3 molecule^{-1} s^{-1}), due to the latter having endothermic barriers for both reaction channels (π-ligand exchange barrier was not calculated for the thiiranium ion as it was not an observed reaction channel, whilst the relative enthalpy for the transition state for addition was +6.2 kJ mol^{-1} at M06-2X/def2-TZVP).[26] This change is reflective of both the increased electrophilicity of the selenium atom compared to the sulfur for π-ligand exchange, and the lower energy $\sigma^*_{CH2\text{-}Se}$ orbital leading to a lower energy ion-molecule association complex for addition (sulfur: -26.3; selenium: -29.4 kJ mol^{-1}).

Table 2. Relative enthalpies for the π-ligand exchange reaction of aryl substituted phenylseleniranium ions **14c-18c** with *cis*-cyclooctene calculated at M06-2X-D3/def2-TZVP (in kJ mol^{-1} at 298 K).

No.	Aryl	ΔH_d	$\Delta H^‡_e$	ΔH_f	ΔH_g	$\Delta\Delta H^‡_\pi$ [b]
15	*m*-$NO_2C_6H_4$	-44.0[a]	-25.7	-76.5[a]	-58.1	+18.3
16	*p*-$CF_3C_6H_4$	-42.5	-22.4	-73.8	-55.9	+20.1
17	*p*-BrC_6H_4	-40.7	-19.3	-71.0	-53.8	+21.5
14	C_6H_5	-39.8	-17.2	-69.4	-52.5	+22.6
18	*p*-$OMeC_6H_4$	-37.6	-13.8	-65.9	-50.1	+23.8

[a] There is an insignificant difference (at most 1 kJ mol^{-1}) in the relative enthalpies of the complexes if the *m*-NO_2 substituent is *syn* or *anti* with respect to the alkene, but only the **15**-*anti* enthalpies are reported here for clarity (refer to the SI for the **15**-*syn* structures). [b] $\Delta\Delta H^‡_\pi = \Delta H^‡_e - \Delta H_d$

Table 3. Relative enthalpies for the addition reaction of aryl substituted phenylseleniranium ions **14c-18c** with *cis*-cyclooctene calculated at M06-2X-D3/def2-TZVP (in kJ mol^{-1} at 298 K).

No.	Aryl	ΔH_h	$\Delta H^‡_i$	ΔH_j	ΔH_k	$\Delta H^‡_l$	ΔH_m	$\Delta\Delta H^‡_A$ [b]
15	*m*-$NO_2C_6H_4$ [a]	-32.5	-14.2	-75.5	-77.4	-79.9	-211	+18.3
16	*p*-$CF_3C_6H_4$	-31.3	-11.0	-56.6	-72.3	-74.5	-206	+20.3
17	*p*-BrC_6H_4	-30.1	-6.8	-47.9	-65.0	-66.8	-204	+23.3
14	C_6H_5	-29.4	-4.0	-42.8	-61.5	-63.4	-203	+25.4
18	*p*-$OMeC_6H_4$	-27.9	+0.4	-35.0	[c]	-54.2	-200	+28.3

[a] There is an insignificant difference (less than 2 kJ mol^{-1}) at the ring-opening step $\Delta H^‡_i$ if the *m*-NO_2 substituent is *syn* or *anti* with respect to the alkene, however, the *anti* conformation leads to a subsequently lower energy pathway and so only the **15**-*anti* enthalpies are reported here (refer to the SI for the **15**-*syn* structures). [b] $\Delta\Delta H^‡_A = \Delta H^‡_i - \Delta H_h$ [c] **18k** was not located as IRC calculations on the ring-closing transition state **18l** led to the five-membered ring product **18m**, but also bifurcated to a higher energy six-membered ring product **18m'** involving the electron-rich *ipso* carbon (**Figure S20A**, SI). IRC calculations on the unsubstituted phenyl transition state **14l** still led to **14k** and **14m** as indicated (**Figure S20B**, SI).

This analysis was extended to the substituted aryl derivatives for both the π-ligand exchange and addition channels. Compared to the phenyl system, increasing the electrophilicity of the seleniranium ion both stabilises the ion-molecule complexes and lowers the transition state barriers for each pathway (**Table 2** and **Table 3**). For π-ligand exchange, there is a small change in the relative energy of the association complex from the most electron withdrawing *m*-nitro to the most electron donating *p*-methoxy substituent of around 8 kJ mol^{-1}. There is a slightly larger change in relative energy at the

transition state of 12 kJ mol^{-1}, which translates into the difference between the association complex and transition state, i.e. the energy change at the rate determining step ($\Delta\Delta H^{\ddagger}_{\pi}$), decreasing slightly (approximately 4-5 kJ mol^{-1} depending on the orientation of the *m*-nitro) as the selenium becomes more electron deficient.[42] However, the same examination of the addition pathway shows a much larger change at the transition state moving from the *p*-methoxy to *m*-nitro substituents. In particular, the key ring opening transition state decreases in relative energy by 16.2 kJ mol^{-1}, whilst the complex immediately prior to this transition state decreases by only a few kilojoules per mole. This means that the $\Delta\Delta H^{\ddagger}_{A}$ shows a much larger change of 12 kJ mol^{-1}, around three times more than the π-ligand exchange pathway, as the seleniranium ion becomes more electrophilic. This suggests that the addition pathway should be increasingly favoured over the π-ligand exchange pathway as the aryl substituent becomes more electron withdrawing.

Table 4. Experimental branching ratios (BR) for ion-molecule reactions of aryl substituted seleniranium ions **14c-18c** with *cis*-cyclooctene

			π-Ligand Exchange		**Addition**	
No.	**Aryl**	***m/z***	**BR[a]**	***m/z***	**BR[a]**	***m/z***
15c	*m*-$NO_2C_6H_4$	230	0.74 ± 0.02	312	0.26 ± 0.02	340
16c	*p*-$CF_3C_6H_4$	253	0.85 ± 0.01	335	0.15 ± 0.01	363
17c	*p*-BrC_6H_4	263	0.91 ± 0.004	345	0.09 ± 0.004	373
14c	C_6H_5	185	0.97 ± 0.02	267	0.03 ± 0.02	295
18c	*p*-$OMeC_6H_4$	215	0.98 ± 0.002	297	0.02 ± 0.002	325

[a] Errors are given as one standard deviation from at least five independent measurements, though a conservative error is ± 20%.[34]

The change in reaction partitioning predicted by the calculations is qualitatively observed in the mass spectra shown in **Figure 2**, where the stronger electron withdrawing groups (*m*-NO_2 and *p*-CF_3, **A** and **B** respectively) have produced more than 25% relative abundance of the addition product, whilst the weaker *p*-Br (**C**) and the electron donating *p*-OMe (**D**) show less than 25% of the addition product. To quantify the relative amounts of the π-ligand exchange and addition products produced, the branching ratios (BR) were determined by extrapolating the change in each product ion intensity as a proportion of the total change in product ion count to zero time to correct for the presence of the more reactive isomer (see SI **Figure S21**). As shown in **Table 4**, there is an increase in the branching ratio for π-ligand exchange as the phenyl substituent on the selenium becomes more electron donating: *m*-$NO_2C_6H_4$ (0.74) < *p*-$CF_3C_6H_4$ (0.85) < *p*-BrC_6H_4 (0.90) < C_6H_5 (0.97) < *p*-$OMeC_6H_4$ (0.98), whilst there is a concomitant decrease in the addition branching ratio (*m*-$NO_2C_6H_4$ = 0.26 *vs* *p*-$OMeC_6H_4$ = 0.02). A Hammett plot of the branching ratios shows a relatively linear relationship with an R^2 value of 0.88 reinforcing the earlier solution phase work with addition at the iranium carbon being favoured over attack at the selenium as the aryl substituent becomes more electron withdrawing (**Figure 6**). The electron donating *p*-methoxyphenyl group in **18** significantly deactivates the iranium carbons to nucleophilic attack (only 2% addition) and instead favours attack at selenium (98% π-ligand exchange), which qualitatively agrees with the low 5% enantiospecificity obtained for the tetrahydrofuran product **9** (aryl = *p*-$OMeC_6H_4$) in Denmark's study (**Scheme 2**).[9] However, there is still significant partitioning towards the π-ligand exchange pathway with the *p*-trifluoromethyl substituent in **16** (85%), reflective of a tetrahydrofuran **9** (aryl = *p*-$OMeC_6H_4$) with only 27% es following ring opening of the corresponding carbonate **7**. Further, given that the π-ligand exchange pathway is still dominant even with the strongly electron withdrawing *m*-nitro substituent in **15** supports the earlier contention that the best aryl substituents to sustain optical purity in reactions proceeding *via* seleniranium ions are those *ortho* to the selenium that exhibit a strong steric influence and/or a through-space interaction that blocks incoming nucleophilic attack at the selenium.

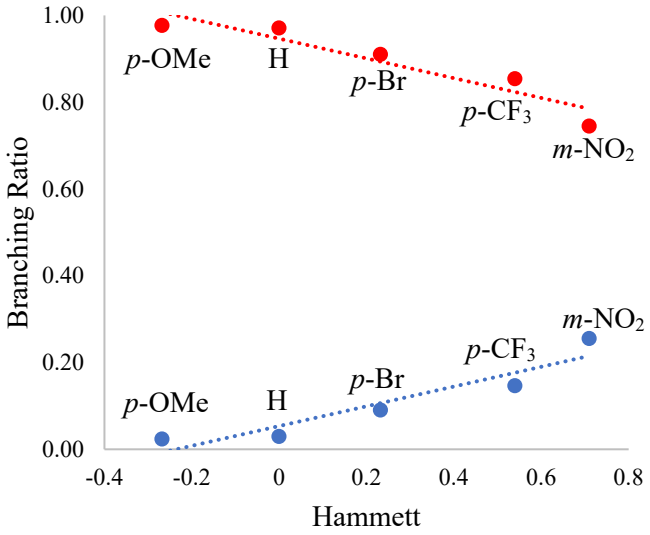

Figure 6. Hammett plot for the branching ratios of π-ligand exchange (red) and addition (blue) pathways from reaction of *cis*-cyclooctene with seleniranium ions **14c-18c**. $R^2 = 0.88$.

As mentioned, for some species there appeared to be an isomer that favoured addition being present in larger quantities than the seleniranium ion at first, but over time was consumed leaving the latter as the primary ion present. As discussed in previous work,[25, 26] the most feasible alternative is a selenonium ion that will exclusively undergo addition as it does not meet the geometric requirements for selenium atom transfer in π-ligand exchange.[28, 43, 44] The prior studies established that the thiiranium and seleniranium ions were the dominant ion present, though it was difficult to rule out the minor presence of an -onium ion with the experimental and theoretical techniques used. To investigate this experimentally, the early onset of the reaction of the *m*-nitrophenyl, *p*-trifluoromethylphenyl, and phenylseleniranium ions **14c-16c** with *cis*-cyclooctene were examined in greater detail by lowering the concentration of the alkene. As shown in **Figure 7A**, the addition product **14m** (*m/z* 295, blue triangles) increases more rapidly than the π-ligand exchange product **14g** (*m/z* 267, red circles) at first, but plateaus leading to a shift in the partitioning by 400 ms. This phenomenon is present to a lesser extent for the *p*-trifluoromethylphenylseleniranium ion **16c**, but not at all for the *m*-nitrophenylseleniranium ion **15c** (see SI **Figure S18**). This is reflected in the plot of ln[(precursor ion intensity)/(total ion intensity)] *vs* reaction time with non-linear behaviour at early reaction times reflecting the presence of the more reactive selenonium ion (**Figure 7B**). Indeed, the thiiranium ion congener has been shown to react over 260 times slower than an independently generated sulphonium ion,[26] and so the initially fast kinetics observed supports the proposed selenonium ion impurity (DFT calculations also support a barrierless pathway for addition of *cis*-cyclooctene to the selenonium ion with $\Delta\Delta H^{\ddagger} = -0.3$ kJ mol^{-1}, see **Figure S22** in the SI). However, the challenge in this explanation is reasoning why *only* the unsubstituted phenyl species leads to a substantial amount of isomerisation, and that a trend is not apparent as the electron demand changes on the selenium (*c.f.* product ion ratios in **Figure 1** with those in **Figure 2**).

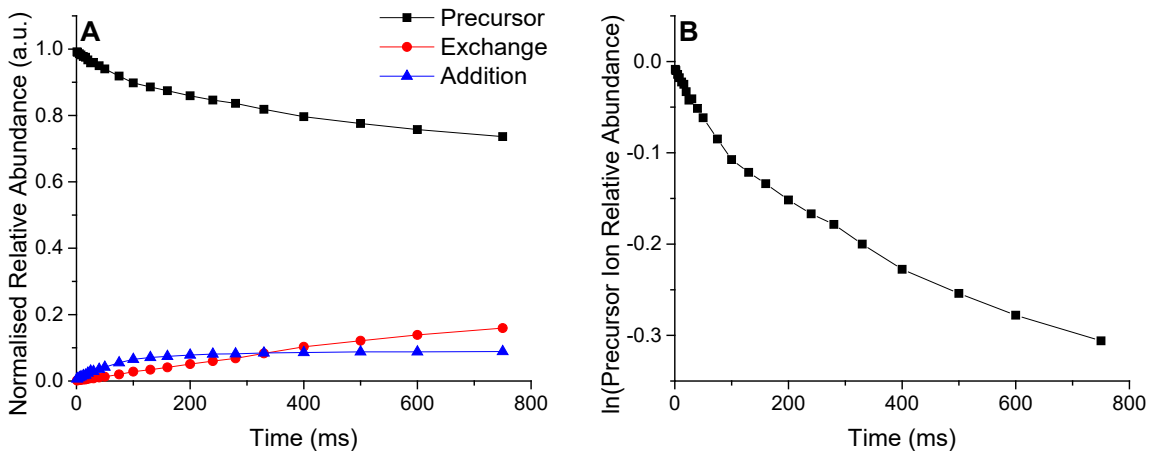

Figure 7. Early onset of the IMR between phenylseleniranium ion **14c** and *cis*-cyclooctene (5.3×10^{10} molecule cm^{-3}) (**A**) kinetic curves of the relative abundances of the precursor ion **14c** (*m/z* 185, black squares), π-ligand exchange product **14g** (*m/z* 267, red circles) and addition product **14m** (*m/z* 295, blue triangles) (**B**) plot of ln(precursor ion relative abundance) against reaction time (ms) used to determine *pseudo* first order rate coefficients showing non-linear behaviour at early reaction times.

To investigate how changing the substitution on the phenyl ring affects isomerisation, the key hydride transfer transition state for this process and the selenonium product ions were calculated for three of these species (**Scheme 6C**). However, not only are the barriers very high to isomerisation ($\Delta H^{\ddagger} > 200$ kJ mol^{-1} relative to the iranium ion), which is unsurprising given that a substantial amount of positive charge builds up on a primary carbon prior to hydride transfer, but there is no thermodynamic driving force towards selenonium ion formation for any of these species ($\Delta H > 25$ kJ mol^{-1}). Potential isomerisation was also considered during CID as around 70-80 kJ mol^{-1} is required to displace the ammonia and the overall formation of the seleniranium ion is endothermic (**Scheme 6A**).[45] However, the transition state for the 1,2-hydride shift to the selenonium ion with the ammonia present is still more than double that of the formation of the seleniranium ion at 177-184 kJ mol^{-1} (**Scheme 6B**), in agreement with previous DFT calculations for a similar seleniranium ion system.[25] The barriers and endothermicities of the unimolecular reactions all increase as the electron demand on selenium increases as the 1,2-hydride shift is assisted by the selenium atom lone pair, which becomes less nucleophilic as the substituent on the phenyl ring becomes more electron withdrawing. We did consider whether mass selecting the iranium ion in an MS^2 experiment following in-source decomposition of the ammonium precursor **b** would lead to less isomerisation. However, the subsequent ion-molecule reaction of the phenylseleniranium **14c** with *cis*-cyclooctene showed approximately 30% more relative abundance of the addition product ion than the corresponding MS^3 experiment (see **Figure S23** in the SI). This is likely due to other bimolecular isomerisation pathways becoming available from solvent assistance such as Hofmann elimination leading to the selenonium ion *via* a solvent mediated proton transport mechanism (formally a 1,2-hydride shift).[46] Any mechanism in the ESI source would also benefit from solvent stabilising charges along the reaction pathway, significantly lowering potential barriers to isomerisation. Given that the MS^3 experiments suggested less isomerisation during CID, only the calculations reflecting the processes available in the ion trap were considered and these do not suggest the unsubstituted phenyl system as an outlier for isomerisation.[32]

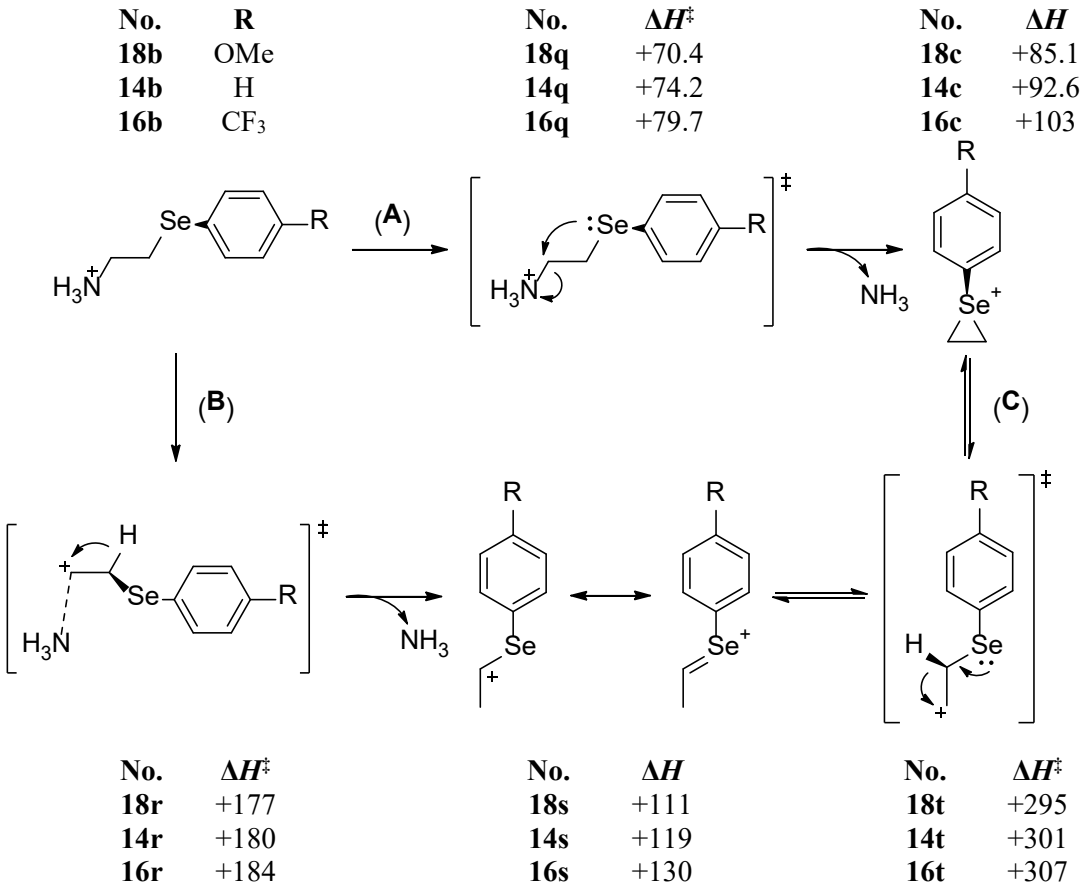

Scheme 6. Effect of changing electron demand at selenium on relative enthalpies for (**A**) displacement of ammonia *via* **q** to give the seleniranium ion **c**,[45] (**B**) displacement of ammonia *via* **r** to give the selenonium ion **s** (a *syn* elimination transition state **14r'** was also found, but was higher in relative enthalpy at +211 kJ mol^{-1}) and (**C**) isomerisation of seleniranium ion **c** to selenonium ion **s** *via* a 1,2-hydride shift in **t**. Enthalpies (ΔH) are relative to the corresponding ammonium ion **b** precursor for each substituent (R = OMe, H, and CF_3), and are in kJ mol^{-1} at 298 K calculated at M06-2X-D3/def2-TZVP.

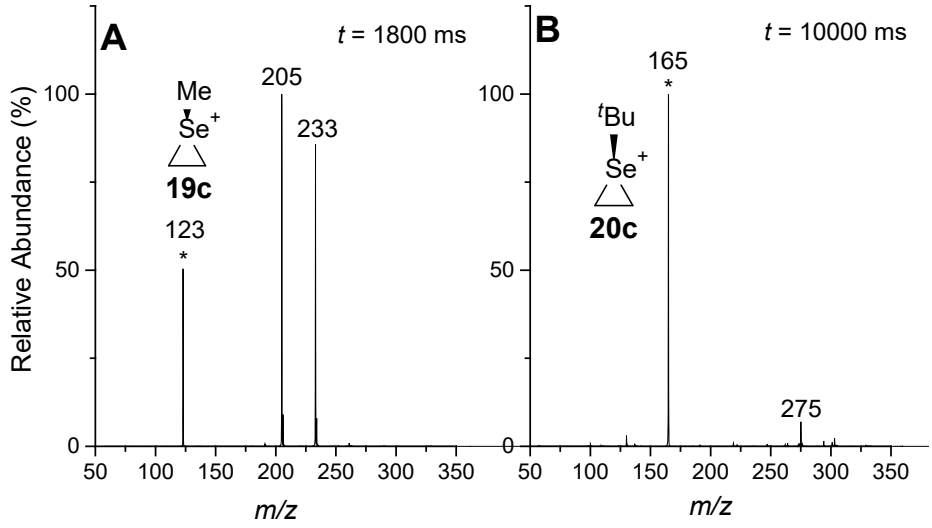

Figure 8. MS^3 IMR of *cis*-cyclooctene with (**A**) methylseleniranium ion **19c** (*m/z* 123, *) to give π-ligand exchange product **19g** (*m/z* 205) and addition product **19m** (*m/z* 233) at *t* = 1800 ms with [*cis*-cyclooctene] = 5.3 × 10^{11} molecule cm^{-3}, (**B**) *t*-butylseleniranium ion **20c** (*m/z* 165, *) to give addition

product **20m** (*m/z* 275) at *t* = 10000 ms with [*cis*-cyclooctene] = 1.1 × 10^{12} molecule cm^{-3} (a higher concentration of the neutral was required due to the very low reactivity of *m/z* 165). The most abundant ^{80}Se isotope was mass-selected (*). See **Figure S26A** in the SI for HRMS (note that HRMS was unable to obtained for IMR of **20c**)

Following the electronic effects on the seleniranium ion reactivity with *cis*-cyclooctene, steric effects were also explored. As discussed above, several studies have shown that increasing the steric bulk at the selenium can hinder the approach of incoming nucleophiles, thus disfavouring π-ligand exchange.[9, 15, 16] To examine this effect in the gas phase, the reactivity of seleniranium ions with methyl and *tert*-butyl substituents on the selenium was explored. **Figure 8** shows the IMR spectra for the *Se*-methyl- and *Se*-*t*-butyl-substituted seleniranium ions **19c** and **20c** respectively with *cis*-cyclooctene. Changing the phenyl (**Figure 1**) to a methyl group (**Figure 8A**) shifts the partitioning towards addition and may be rationalised by an increase in apparent steric bulk from the flat phenyl group to the tetrahedral methyl group, which hinders the approach of the alkene. This steric change also outcompetes any change from the slightly electron withdrawing sp^2 hybridised phenyl carbon to the more electron donating sp^3 methyl carbon, as the latter would be expected to favour π-ligand exchange based on the above discussion on electronic effects (**Table 4** and **Figure 6**). Further increasing the steric bulk to the *t*-butyl substituent, however, has a dramatic effect on both pathways, shutting down π-ligand exchange (*m/z* 247 not observed), but also significantly slowing down the rate of addition as evidenced by the long reaction time required to observe any significant product formation (**Figure 8B**). Due to the very slow reactivity of **20c**, even at high concentrations of *cis*-cyclooctene and long reaction times, accurate kinetics were unable to be determined for this species.

Table 5. Relative enthalpies for the π-ligand exchange reaction of seleniranium ions **14c**, **19c**, and **20c** with *cis*-cyclooctene calculated at M06-2X-D3/def2-TZVP (in kJ mol^{-1} at 298 K).

No.	R	ΔH_d	$\Delta H^{\ddagger}_e$	ΔH_f	ΔH_g	$\Delta\Delta H^{\ddagger}_{\pi}$
14	C_6H_5	-39.8	-17.2	-69.4	-52.5	+22.6
19	CH_3	-44.6	-12.3	-73.1	-55.4	+32.3
20	*t*-Bu	-34.3	+23.4	-61.6	-48.1	+57.7

Table 6. Relative enthalpies for the addition reaction of seleniranium ions **14c**, **19c**, and **20c** with *cis*-cyclooctene calculated at M06-2X-D3/def2-TZVP (in kJ mol^{-1} at 298 K).[a]

No.	R	ΔH_h	$\Delta H^{\ddagger}_i$	ΔH_j	ΔH_m	$\Delta\Delta H^{\ddagger}_A$
14	C_6H_5	-29.4	-4.0	-42.8	-203	+25.4
19	CH_3	-32.1	-7.0	-40.7	-213	+25.2
20	*t*Bu	-28.7	+10.7	-16.6	-206	+39.4

[a] ring closure transition state was not calculated

DFT calculations support these observations with the bulky *t*-butyl group making the kinetic barrier for π-ligand exchange **20e** prohibitively high in the gas phase at +23.4 kJ mol^{-1},[26, 27] whilst the methyl substituent only increases the relative barrier **19e** by 5 kJ mol^{-1} compared to phenyl **14e** (**Table 5**). However, when the enthalpy change from the association ion-molecule complex **d** to the transition state **e** is considered ($\Delta\Delta H^{\ddagger}_{\pi}$: Ph = +22.6; Me = +32.3 kJ mol^{-1}), then the change in the rate-determining barrier is closer to 10 kJ mol^{-1}. The relative enthalpies for the addition pathway also explain the methyl substituent favouring addition over π-ligand exchange compared to the phenyl substituent (**Table 6**). Whilst the former raised the barrier to π-ligand exchange **19e**, it also lowered the barrier to addition **19i** such that the enthalpy from the complex **h** to the ring-opening transition state **i** ($\Delta\Delta H^{\ddagger}_A$) was the same within error for both methyl (+25.2 kJ mol^{-1}) and phenyl (+25.4 kJ mol^{-1}). By comparison, the *t*-butyl group also raised the barrier to addition to +10.7 kJ mol^{-1} above the separated reactants and required longer reaction times (10,000 ms) and much higher *cis*-cyclooctene concentrations (around double compared to methyl) to observe the product *m/z* 275 formation. Even though the transition state is

endothermic, the Boltzmann distribution of ions means that some ions will have enough energy to overcome such barriers of *ca*. 9-10 kJ mol^{-1} at room temperature in the gas phase,[47] albeit with very slow kinetics. As the steric bulk of the *t*-butyl group is unlikely to significantly impact ring opening at the iranium endocyclic carbon, then the higher barrier may be reflective of the greater electron-donating inductive effect of a *t*-butyl compared to a methyl,[48] thus achieving little addition as the iranium carbon is now less electrophilic (*c.f. p*-methoxyphenyl substituent **18**, **Figure 2D** and **Table 3**).

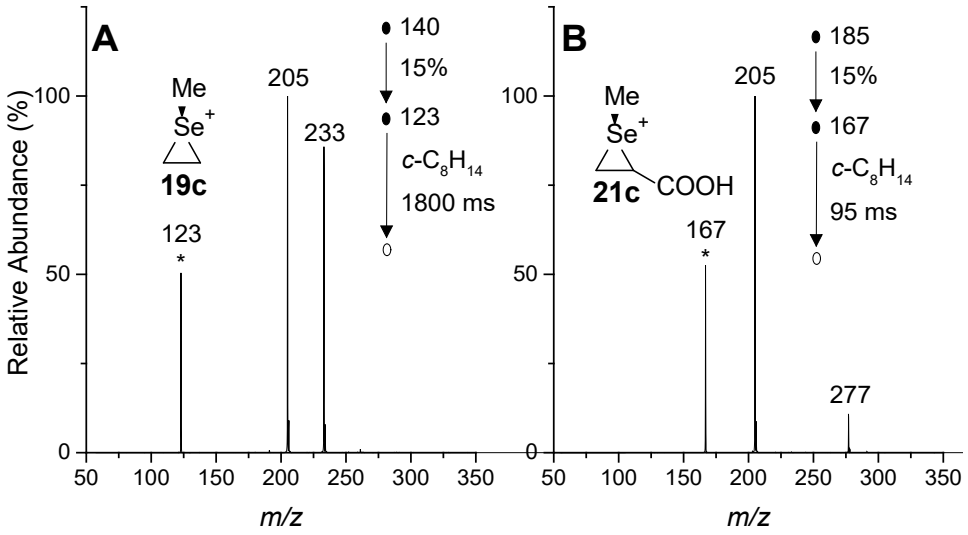

Figure 9. MS^3 IMR of *cis*-cyclooctene with (**A**) methylseleniranium ion **19c** (*m/z* 123, *) to give π-ligand exchange product **19g** (*m/z* 205) and addition product **19m** (*m/z* 233) at *t* = 1800 ms, (**B**) methylselenocysteine iranium ion **21c** (*m/z* 167, *) to give π-ligand exchange product **19g** (*m/z* 205) and addition product **21m** (*m/z* 277) at *t* = 95 ms. [*cis*-cyclooctene] = 5.3 × 10^{11} molecule cm^{-3}. The most abundant ^{80}Se isotope of **19c** and **21c** was mass-selected following CID (NCE of 15%) of ammonium ions **19b** (*m/z* 140) and **21b** (*m/z* 185). See **Figure S26** in the SI for HRMS.

Table 7. Experimental second order rate coefficients (k_2), theoretical collision rate coefficients from average dipole orientation theory (k_{ADO}), reaction efficiency (φ), and branching ratios (BR) for ion-molecule reactions of methylseleniranium ions **19c** and **21c** with *cis*-cyclooctene

					π-Ligand Exchange		**Addition**	
No.	***m/z***	**k_2 (× 10^{-11})^{a,b}**	**k_{ADO} (× 10^{-9})^{a}**	**φ (%)^{c}**	**BR^{b}**	***m/z***	**BR^{b}**	***m/z***
19c	123	0.12 ± 0.008	1.17	0.1	0.55 ± 0.006	205	0.46 ± 0.006	233
21c	167	1.82 ± 0.11	1.10	1.7	0.91 ± 0.002	205	0.09 ± 0.002	277

[a] Units of rate coefficients are cm^3 molecule^{-1} s^{-1}. [b] Errors are given as one standard deviation from at least five independent measurements, though a conservative error is ± 25% (k_2) or ± 20% (BR).[34] [c] φ = (k_2/k_{ADO}) × 100 %. Kinetic curves and branching ratio plots are provided in SI **Figures S27-S29**.

Previous studies have shown that the biologically relevant *S*-methylcysteine will fragment under CID conditions to give the thiiranium ion as a major product,[49] and so we sought to compare the reactivity of the *Se*-methylselenocysteine iranium ion **21c** (*m/z* 167) congener towards *cis*-cyclooctene with that of methylseleniranium ion **19c** (*m/z* 123). The key difference between the two ions is the nature of the substituents attached to the iranium carbons with the former having a carboxylic acid functional group in place of a hydrogen. The mass spectra of these two ion-molecule reactions are shown in **Figure 9** and display a significant shift in the reaction partitioning. Where π-ligand exchange **19g** (*m/z* 205) slightly outcompeted addition **19m** (*m/z* 233) for the methylseleniranium ion **19c** *m/z* 123 (**Figure 9A**), it was the dominant pathway for seleniranium ion **21c** (*m/z* 167) giving **19g** (*m/z* 205) with the addition product **21m** (*m/z* 277) now in only 10-15% relative abundance (**Figure 9B**). Not only do the product ratios differ, the second order rate coefficients show an order of magnitude difference with the rate

increasing for consumption of **19c** (k_2 = 0.12 × 10^{-11} cm^3 $molecule^{-1}$ s^{-1}) to **21c** (k_2 = 1.82 × 10^{-11} cm^3 $molecule^{-1}$ s^{-1}) as shown in **Table 7**. The greater reactivity of the latter ion is reflected in the DFT calculations with the relative enthalpic barriers lowering for both π-ligand exchange (**19e**: -12.3 *vs* **21e**: -24.7 kJ mol^{-1}) and the ring-opening step for addition (**19i**: -7.0 *vs* **21i/21i'**: -16 to -17 kJ mol^{-1}) (**Table 5**, **Table 6** and **Figure 10**). The partitioning change moving from **19** to **21** is explained by the key $\Delta\Delta H^{\ddagger}$ decreasing the most for π-ligand exchange (**19**: +32.3 *vs* **21**: +22.7 kJ mol^{-1}), whilst for addition it changes by 3-4 kJ mol^{-1}, increasing if *cis*-cyclooctene attacks at the carboxy substituted carbon (**19**: +25.2 *vs* **21'**: +28.1 kJ mol^{-1}) or decreasing if at the methylene carbon (**19**: +25.2 *vs* **21**: +21.5 kJ mol^{-1}). Thus, the net change in relative enthalpies favour increased π-ligand exchange and may be rationalised by the change in leaving group from ethene to acrylic acid, with the latter accepting electron density more effectively and being more stable as a conjugated alkene. The same shift in partitioning is also observed comparing the results here for the phenylseleniranium ion *m/z* 185 reactivity (0.31 × 10^{-11} cm^3 $molecule^{-1}$ s^{-1}) with the greater reactivity also favouring π-ligand exchange for the previously studied styryl phenylseleniranium ion *m/z* 261 (4.4 × 10^{-11} cm^3 $molecule^{-1}$ s^{-1}) with *cis*-cyclooctene (**Scheme 3b**), where the change in leaving group is from ethene to styrene.[25]

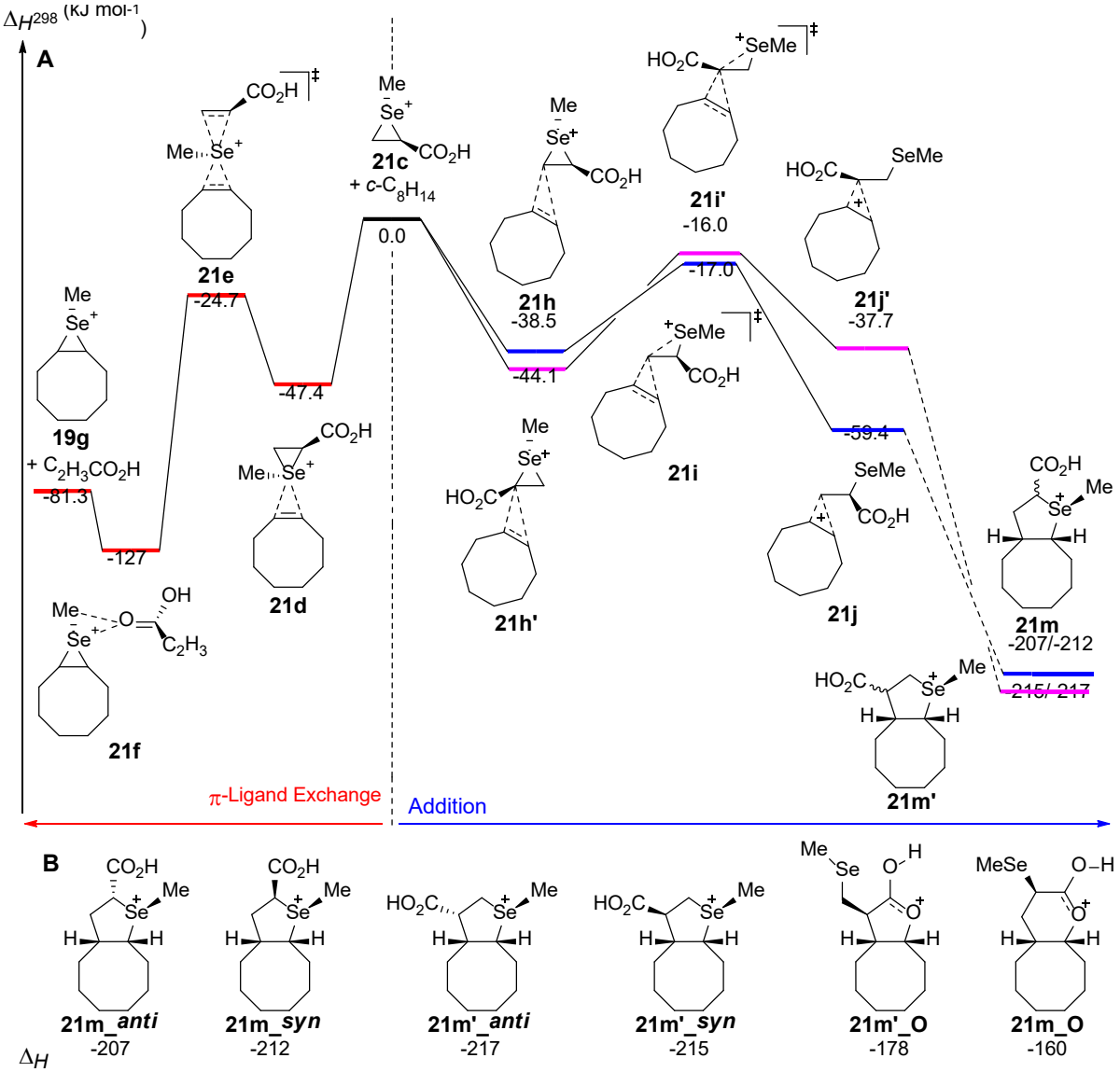

Figure 10. (**A**) Relative enthalpy diagram for ion-molecule reaction of *Se*-methylseleniranium ion **21c** (*m/z* 167) with *cis*-cyclooctene proceeding *via* π-ligand exchange (red) to give **21g** (*m/z* 205) or addition at the methylene carbon (blue) or carboxy substituted carbon (purple) to give **21m** or **21m'** respectively

(*m/z* 277). (**B**) Relative enthalpies for the *syn* and *anti* selenonium ions **21m** or **21m'**, furanylium ion **21m'_O** or pyrylium ion **21m_O** products from addition of *cis*-cyclooctene to **21c**. Enthalpies (ΔH) in kJ mol^{-1} at 298 K are calculated at M06-2X-D3/def2-TZVP. Note in **21f** that acrylic acid is weakly bound to the seleniranium ion in a different orientation to ethene in the other dissociation complexes (**14f-20f**) as confirmed by IRC calculations.

CONCLUSIONS

The reactivity of arylseleniranium ions **14c-18c**, generated by electrospray ionisation (ESI) from the corresponding 2-arylselenylethanamines **14a-18a** and subsequent collision-induced dissociation (CID) of the ammonium ions **14b-18b**, undergoing ion-molecule reactions (IMR) with *cis*-cyclooctene was investigated in the gas phase with a modified linear ion trap mass spectrometer. By varying the substituents on the phenyl ring, the electronic effects upon the reaction rate were explored and gave second order rate coefficients (in cm^3 $molecule^{-1}$ s^{-1}) that increased in the order *p*-$OMeC_6H_4$ **18c** (k_2 = 0.17×10^{-11}) < C_6H_5 **14c** ($k_2 = 0.31 \times 10^{-11}$) < *p*-$BrC_6H_4$ **17c** ($k_2 = 1.11 \times 10^{-11}$) < *p*-$CF_3C_6H_4$ **16c** (k_2 = 2.73×10^{-11}) < *m*-$NO_2C_6H_4$ **15c** ($k_2 = 7.35 \times 10^{-11}$). Further examination of the kinetic curves at early reaction times of the unsubstituted phenyl and *p*-trifluoromethylseleniranium ions **14c** and **16c** did reveal the presence of a more reactive selenonium ion isomer. DFT calculations were unsuccessful at elucidating why only some of the ions showed this behaviour, however, and so the reaction rate coefficients and branching ratios were determined at later reaction times following consumption of the isomer impurity. A Hammett plot of the rates relative to the unsubstituted system gave a linear correlation (R^2 = 0.98) with a ρ of + 1.66 indicating that as the electron demand increased on the selenium, the precursor ion was consumed at a faster rate. This was postulated to be due to both major reaction pathways being favoured as the substituent on the phenyl ring became more electron withdrawing.

To quantify this, branching ratios (BR) were determined for the two reaction pathways: π-ligand exchange, resulting from attack of the alkene at selenium, and addition, resulting from attack at carbon to ring-open the seleniranium ion. The proportion of π-ligand exchange decreased as the substituent became more electron withdrawing (*p*-methoxyphenyl: 98% *vs m*-nitrophenyl: 74%), whilst addition increased (*p*-methoxyphenyl: 2% *vs m*-nitrophenyl: 26%). This was rationalised by DFT calculations at the M06-2X-D3/def2-TZVP level of theory, which suggested that, though making the selenium more electrophilic did lower the kinetic barrier to π-ligand exchange (around 4-5 kJ mol^{-1}), the ring-opening transition state towards addition decreased more in energy (12 kJ mol^{-1}), thus favouring the latter pathway. These results agreed with solution phase studies by Toshimitsu's and Denmark's groups on the electronic effects on a seleno-Ritter and carbonate ring opening reactions respectively that proceed *via* a seleniranium ion from enantioenriched starting materials.[9, 16] Racemisation of the product was largely attributed to attack by nucleophiles at the selenium of the iranium ion intermediate and was suppressed using more electron withdrawing substituents to weaken the selenium-carbon bond of the iranium ion favouring ring-opening. This work demonstrates the ability of gas phase ion-molecule reactions to investigate the reactivity of these types of iranium ions with various nucleophiles, where branching ratios enable translation of the gas phase reactivity to predict solution phase configurational stability.

The sensitivity of the seleniranium ions to steric effects were explored by changing the R group on the selenium from the flat phenyl substituent in **14c** to a tetrahedral methyl group in **19c**. This change shifted the reaction partitioning towards addition as the barrier to π-ligand exchange increased. However, further increasing the steric bulk by employing a *t*-butyl group significantly reduced the reactivity of the seleniranium ion **20c** with only a minor amount of addition and no π-ligand exchange observed. Finally, the reactivity of the iranium ion **21c** derived from CID of the biologically relevant molecule *Se*-methylselenocysteine was examined. Changing one of the hydrogens on the iranium carbons of **19c**

to a carboxylic acid in **21c** lowered the barrier to π-ligand exchange as the leaving group was changed from ethene to the conjugated acrylic acid. This led to both a significant in the branching ratio for π-ligand exchange and the second-order rate coefficient for **21c** compared to **19c**.

EXPERIMENTAL AND THEORETICAL METHODS

Experimental

Reagents and synthesis: The following reagents were used as received for mass spectrometry experiments: *cis*-cyclooctene (95%, Alfa Aesar); *Se*-(methyl)selenocysteine hydrochloride **21a** (≥95%, Sigma-Aldrich). 2-Selenylethanamines **14a-20a** were synthesised from commercially available reagents as detailed in the Supporting Information.

Mass Spectrometry. Multistage mass spectrometry (MS^n) experiments were carried out using a commercially available hybrid dual-pressure linear quadrupole ion trap (LTQ Velos Pro) and Orbitrap Elite mass spectrometer (Thermo Scientific).[50-52] The substituted 2-selenylethanamines **14a-20a** as *ca* 0.1 mM solutions in methanol and *Se*-(methyl)selenocysteine hydrochloride **21a** as *ca* 0.1 mM solution in 50:50 methanol/water were introduced into the electrospray ionisation (ESI) source, operating in positive ion mode, *via* a syringe pump operating at a rate of 5 μL min^{-1}. The source conditions were tuned to optimise the substituted 2-selenylethanammonium ion **14b-21b** signal with typical ESI conditions involving a heated capillary temperate of 250 ºC with an applied voltage of 3.0-4.0 kV; sheath gas flow 10 (arbitrary units); RF lens 60-70%, and other parameters were tuned to maximize the desired peak. The injection time was set using the automatic gain control (AGC) function. All mass spectra presented in this manuscript are an average of at least 100 scans, except for the IMR spectra of ions **18c** and **19c** which were an average of at least 50 scans. The ammonium precursor ions **14b-21b** were mass selected with a window of 5 Da in a MS^2 experiment and then subjected to collision induced dissociation (CID) using a corresponding normalized collision energy (NCE) of 15% (arbitrary units) and collisional activation Q (dimensionless parameter of the Mathieu equation) of 0.25 for a period of 10 ms to generate the seleniranium ions **14c-21c**. All high-resolution mass spectrometry (HRMS) experiments were carried out on the same instrument for all CID and IMR experiments with the ions sent from the LTQ to the Orbitrap MS for analysis to generate the high-resolution tandem mass spectra.

Ion-Molecule Reactions. The seleniranium ions **14c-21c** were mass selected with a window of 2 Da in a MS^3 experiment (^1H, ^{12}C, ^{16}O, ^{14}N, ^{19}F or ^{80}Se, noting that the *p*-bromophenylseleniranium ion **17c** was a mixture of $^{79}Br/^{80}Se$ and $^{81}Br/^{78}Se$) and allowed to react with *cis*-cyclooctene, that had been introduced into the mass spectrometer *via* the helium bath gas line, in ion-molecule reactions (IMR). The modifications to the instrument to allow the study of IMR has been described previously in detail for the current set up.[34] Under ion-molecule conditions (NCE of 0%, low Q values of 0.25, and reaction time varied between 0.03 ms and 10,000 ms prior to ejection from the ion-trap for detection for 1-2 half-lives of the reactant ion), collisions with the helium bath gas quasi-thermalize the ions in LTQ ion-traps (318 ± 23 K),[53] noting that the pressure of the region where the ion-molecule reactions occur in the current set up is 5 mTorr.[52] The relative abundance of the reactant ion was determined by integrating the area under a specified *m/z* region (±0.5 Da) and normalizing it to the integrated signal over the entire spectrum (*m/z* 50-500), and then averaged over all scans for a given reaction time at a particular alkene concentration. The procedure to determine the second order rate coefficients and reaction efficiencies has been described in detail previously.[34] Briefly, taking the negative of the gradient from a plot of the natural logarithm of the relative abundance of the reactant ion against reaction time yields the *pseudo* first order rate coefficient, k_1 (s^{-1}), and dividing this value by the concentration of the neutral in the ion-trap gives the second order rate coefficient, k_2 (cm^3 $molecule^{-1}$ s^{-1}). This value is averaged across at least 5 independent kinetic measurements taken over several days using different alkene concentrations by varying the neutral flowrate. The calculation of the concentration (number

density) of the neutral species present in the ion-trap is dependent on the measured flowrate of helium gas, rate of injection of the volatile neutral reagent, and pressure in the ion-trap and has been described in detail previously,[34] noting that the conservative error of 25% quoted for the second order rate coefficients is attributed to uncertainty in these values. The reliability of the rate coefficients in this study is supported by the good agreement of the rate coefficient of the relatively slow bimolecular ion-molecule reaction of Br^- with CH_3I determined on the present instrumentation ($k_2 = 2.40 \times 10^{-11}$ cm^3 molecule^{-1} s^{-1}) to those found using flowing afterglow techniques ($k_2 = 2.89 \times 10^{-11}$ cm^3 molecule^{-1} s^{-1}) and in an LCQ quadrupole ion trap ($k_2 = 2.7 \times 10^{-11}$ cm^3 molecule^{-1} s^{-1}).[54, 55] The collision rate coefficient used to determine the reaction efficiency was calculated using the parameterized average dipole orientation (ADO) theory of Su and Bowers,[56-58] implemented in the program COLRATE,[59] using a polarizability of 14.49 amu Å^2 and dipole moment of 0.43 D for *cis*-cyclooctene.[34] Branching ratios are typically determined by taking the relative intensity of a product ion as a proportion of all product ion intensities at various reaction times and extrapolating to $t = 0$ (see reference 34 for more detail), but in this study the change in each product ion intensity as a proportion of the change in total product ion intensity was used. Using the former method, non-linear branching ratio plots were obtained for ion-molecule reactions where the isomeric impurity was present in large amounts (such as reaction of **14c** with *cis*-C_8H_{14}), but the latter method gave plots where only the initial portion was non-linear with removal of this section giving **Figure S21D** in the SI as an example. In cases where the isomeric impurity was not an issue, both methods yielded the same results.

Quantum Chemistry Calculations

Density functional theory (DFT) calculations were performed with the Gaussian 16 revision *C.01* software package.[60] Structures were optimised without symmetry constraints using the hybrid meta-GGA M06-2X functional with Grimme's 2010 dispersion correction (denoted M06-2X-D3) and the def2-TZVP basis set.[61-63] The M06-2X functional is applicable for main group thermochemistry and has been used to study chalcogen iranium ions previously.[26-28, 64] Frequency analysis confirmed all structures were minima (no imaginary frequencies) and intrinsic reaction coordinate (IRC) calculations were used to verify that ambiguous transition state structures were connected to the intermediates. Unless otherwise noted, reaction enthalpies in the text are at 298 K and are corrected with unscaled zero-point vibrational energies (ZPVE). In the gas phase, several studies have shown that thermoneutralised ions (often following radiative dispersal or collisional cooling with bath gas) do not possess sufficient internal energy to overcome barriers higher than that of the system (defined by the combined energy of the free reactants).[35, 36] This leads to the pertinent thermodynamic quantity being the enthalpy rather than Gibbs free energy that accurately describes the potential energy surface of ion-molecule reactions in the gas phase under the low pressure regime employed in this study.[65, 66] Nevertheless, error in calculations (around 5-8 kJ mol^{-1} based on benchmarking studies of the M06-2X functional with similar sized basis sets[64, 67]) and the internal energy that ions possess before they are completely thermoneutral means barriers of around 5-10 kJ mol^{-1} above the reactants energy may be overcome, albeit with very slow rates of reaction.[26, 47]

AUTHOR INFORMATION

Corresponding Authors

*Email: brydons@student.unimelb.edu.au

ORCID

Samuel C. Brydon: 0000-0002-8939-0249

Catriona Thomson: 0000-0002-9328-1109

Richard A. J. O'Hair: 0000-0002-8044-0502

Jonathan M. White: 0000-0002-0707-6257

CONFLICT OF INTEREST

The authors declare no competing financial interest.

ASSOCIATED CONTENT

Data Availability Statement

The data underlying this study are available in the published article and its online supplementary material.

Supporting Information Statement

NMR and synthetic experimental details as well as spectroscopic characterisation for amines **14a-20a**. High-resolution mass spectra for collision-induced dissociation of ammonium ions **14b-21b** and ion-molecule reaction of seleniranium ions **14c-21c** with *cis*-cyclooctene. *Pseudo* first order kinetic plots of the consumption of the precursor seleniranium ion **14c-21c** in the ion-molecule reactions and branching ratio plots for the π-ligand exchange and addition products. Kinetic curves for the early onset of the IMR of ions **15c** and **16c** and at longer reaction times for **19c** and **21c** with *cis*-cyclooctene. IRC calculations on transition states **18l** and **14l**, and the relative enthalpy diagram for IMR of selenonium ion **14s** with *cis*-cyclooctene. Cartesian coordinates and absolute energy values (*E* at 0 K; *H* at 298 K) of all calculated structures.

ACKNOWLEDGMENTS

We thank the Australian Research Council (ARC) for financial support through the Discovery Projects (DP180101187 to RAJO), the Australian Government for Research Training Program (RTP) scholarships to SB and CT, and the Elizabeth and Vernon Puzey Scholarship to CT. Calculations were performed on the Spartan High Performance Computing (HPC) System,[68] hosted by the Research Platform Services at the University of Melbourne. Discussions on the branching ratios and involvement of isomers with Dr Gabriel da Silva are very appreciated.

REFERENCES

(1) Poleschner, H.; Seppelt, K. Seleniranium and Telluriranium Salts. *Chem. Eur. J.* **2018**, *24* (64), 17155-17161.

(2) Denmark, S. E.; Collins, W. R.; Cullen, M. D. Observation of Direct Sulfenium and Selenenium Group Transfer from Thiiranium and Seleniranium Ions to Alkenes. *J. Am. Chem. Soc.* **2009**, *131* (10), 3490-3492.

(3) Ortgies, S.; Breder, A. Oxidative Alkene Functionalizations via Selenium-π-Acid Catalysis. *ACS Catal.* **2017**, *7* (9), 5828-5840.

(4) Singh, F. V.; Wirth, T. Organoselenium Chemistry. In *Encyclopedia of Inorganic and Bioinorganic Chemistry*, Scott, R. A. Ed.; John Wiley & Sons, Ltd, 2018; pp 1-32.

(5) Brydon, S. C.; White, J. M. 1.07 - Three-Membered Rings With One Selenium or Tellurium Atom. In *Comprehensive Heterocyclic Chemistry IV*, Black, D. S., Cossy, J., Stevens, C. V. Eds.; Elsevier, 2022; pp 436-463.

(6) Makhal, P. N.; Nandi, A.; Kaki, V. R. Insights into the Recent Synthetic Advances of Organoselenium Compounds. *ChemistrySelect* **2021**, *6* (4), 663-679.

(7) G, S.; Shetgaonkar, S. E.; Singh, F. V. Recent Advances in Organoselenium Catalysis. *Curr. Org. Synth.* **2022**, *19* (3), 393-413.

(8) Denmark, S. E.; Collins, W. R. Lewis Base Activation of Lewis Acids: Development of a Lewis Base Catalyzed Selenolactonization. *Org. Lett.* **2007**, *9* (19), 3801-3804.

(9) Denmark, S. E.; Kalyani, D.; Collins, W. R. Preparative and Mechanistic Studies toward the Rational Development of Catalytic, Enantioselective Selenoetherification Reactions. *J. Am. Chem. Soc.* **2010**, *132* (44), 15752-15765.

(10) Kalyani, D.; Kornfilt, D. J. P.; Burk, M. T.; Denmark, S. E. Lewis Base Catalysis: A Platform for Enantioselective Addition to Alkenes Using Group 16 and 17 Lewis Acids (n → σ*). In *Lewis Base Catalysis in Organic Synthesis*, Vedejs, E., Denmark, S. E. Eds.; Wiley-VCH, 2016; pp 1153-1212.

(11) Denmark, S. E.; Vogler, T. Synthesis and Reactivity of Enantiomerically Enriched Thiiranium Ions. *Chem. Eur. J.* **2009**, *15* (43), 11737-11745.

(12) Gruttadauria, M.; Aprile, C.; Riela, S.; Noto, R. Synthesis of 2,4,6-trisubstituted tetrahydropyrans via 6-exo selenoetherification of unsaturated alcohols. *Tetrahedron Lett.* **2001**, *42* (11), 2213-2215.

(13) Aprile, C.; Gruttadauria, M.; Amato, M. E.; D'Anna, F.; Lo Meo, P.; Riela, S.; Noto, R. Studies on the stereoselective selenolactonization, hydroxy and methoxy selenenylation of α- and β-hydroxy acids and esters. Synthesis of δ- and γ-lactones. *Tetrahedron* **2003**, *59* (13), 2241-2251.

(14) Wirth, T.; Fragale, G.; Spichty, M. Mechanistic Course of the Asymmetric Methoxyselenenylation Reaction. *J. Am. Chem. Soc.* **1998**, *120* (14), 3376-3381.

(15) Toshimitsu, A.; Nakano, K.; Mukai, T.; Tamao, K. Steric Protection of the Selenium Atom of the Episelenonium Ion Intermediate To Prevent both the Racemization of the Chiral Carbon and the Selenophilic Attack of Carbon Nucleophiles. *J. Am. Chem. Soc.* **1996**, *118* (11), 2756-2757.

(16) Toshimitsu, A.; Nakano, K.; Tamao, K. Prevention of Racemization of the Chiral Carbon in the Episelenonium ION Intermediate: Steric Protection and Electron-Withdrawing Effect. *Phosphorus, Sulfur Silicon Relat. Elem.* **1998**, *136* (1), 649-652.

(17) Toshimitsu, A.; Hirosawa, C.; Nakano, K.; Mukai, T.; Tamao, K. Stereospecific Transformations of Chiral Compounds Using Anchimeric Assistance of Arylthio and Arylseleno Group. *Phosphorus, Sulfur Silicon Relat. Elem.* **1997**, *120* (1), 355-356.

(18) Mukherjee, A. J.; Zade, S. S.; Singh, H. B.; Sunoj, R. B. Organoselenium Chemistry: Role of Intramolecular Interactions. *Chem. Rev.* **2010**, *110* (7), 4357-4416.

(19) Singh, V. P.; Singh, H. B.; Butcher, R. J. Stable Selenenium Cations: Unusual Reactivity and Excellent Glutathione Peroxidase-Like Activity. *Eur. J. Inorg. Chem.* **2010**, *2010* (4), 637-647.

(20) Toshimitsu, A.; Ito, M.; Uemura, S. The stereochemistry of a substitution reaction via an episelenonium ion: retention by a 2-pyridylseleno group versus scrambling by a phenylseleno group. *J. Chem. Soc., Chem. Commun.* **1989**, (9), 530-531.

(21) Okamoto, K.; Nishibayashi, Y.; Uemura, S.; Toshimitsu, A. Stereospecific carbon–carbon bond formation by the reaction of a chiral episelenonium ion with aromatic compounds. *Tetrahedron Lett.* **2004**, *45* (32), 6137-6139.

(22) Potapov, V. A.; Ishigeev, R. S.; Shkurchenko, I. V.; Zinchenko, S. V.; Amosova, S. V. Natural Compounds and Their Structural Analogs in Regio- and Stereoselective Synthesis of New Families of Water-Soluble 2H,3H-[1,3]Thia- and -Selenazolo[3,2-a]pyridin-4-ium Heterocycles by Annulation Reactions. *Molecules* **2020**, *25* (2), 376.

(23) Bock, J.; Daniliuc, C. G.; Bergander, K.; Mück-Lichtenfeld, C.; Hennecke, U. Synthesis, structural characterisation, and synthetic application of stable seleniranium ions. *Org. Biomol. Chem.* **2019**, *17* (12), 3181-3185.

(24) Maji, B. Stereoselective Haliranium, Thiiranium and Seleniranium Ion-Triggered Friedel–Crafts-Type Alkylations for Polyene Cyclizations. *Adv. Synth. Catal.* **2019**, *361* (15), 3453-3489.

(25) Lim, S. F.; Harris, B. L.; Khairallah, G. N.; Bieske, E. J.; Maître, P.; da Silva, G.; Adamson, B. D.; Scholz, M. S.; Coughlan, N. J. A.; O'Hair, R. A. J.; Rathjen, M.; Stares, D.; White, J. M. Seleniranium Ions Undergo π-Ligand Exchange via an Associative Mechanism in the Gas Phase. *J. Org. Chem.* **2017**, *82* (12), 6289-6297.

(26) Brydon, S. C.; Lim, S. F.; Khairallah, G. N.; Maître, P.; Loire, E.; da Silva, G.; O'Hair, R. A. J.; White, J. M. Reactions of Thiiranium and Sulfonium Ions with Alkenes in the Gas Phase. *J. Org. Chem.* **2019**, *84* (16), 10076-10087.

(27) Brydon, S. C.; Ren, Z.; da Silva, G.; Lim, S. F.; Khairallah, G. N.; Rathjen, M. J.; White, J. M.; O'Hair, R. A. J. Experimental and DFT Studies on the Identity Exchange Reactions between Phenyl Chalcogen Iranium Ions and Alkenes. *J. Phys. Chem. A* **2019**, *123* (38), 8200-8207.

(28) Brydon, S. C.; da Silva, G.; White, J. M. Evidence that π-ligand exchange reactions of chalcogen iranium ions proceed via Hückel pseudocoarctate transition states. *J. Phys. Org. Chem.* **2020**, *33* (12), e4111.

(29) Herges, R. Coarctate and Pseudocoarctate Reactions: Stereochemical Rules. *J. Org. Chem.* **2015**, *80* (23), 11869-11876.

(30) Though a β-selenocarbocation 1' would also be an isomer that could undergo addition, this primary carbocation is very unstable and was not found at the current level of theory with attempts to calculate this structure leading to either the iranium or onium ion. Previous studies where a benzylic β-selenocarbocation was more feasible in both sulphur (reference 26) and selenium (reference 25) species have also suggested against such a structure.

(31) Hansch, C.; Leo, A.; Taft, R. W. A survey of Hammett substituent constants and resonance and field parameters. *Chem. Rev.* **1991**, *91* (2), 165-195.

(32) We did consider re-selecting the seleniranium ion in an MS^4 experiment after an appropriate amount of time to titrate out the isomeric impurity, however, this led to further complications as the re-selection process energised the ions sufficently to cause more isomerisation (similar effects have beend observed previously in reference 33). Further discussion and additional results on this are provided in the SI.

(33) Barlow, C. K.; Wright, A.; Easton, C. J.; O'Hair, R. A. J. Gas-phase ion-molecule reactions using regioselectively generated radical cations to model oxidative damage and probe radical sites in peptides. *Org. Biomol. Chem.* **2011**, *9* (10), 3733-3745.

(34) Brydon, S. C.; da Silva, G.; O'Hair, R. A. J.; White, J. M. Experimental and theoretical investigations into the mechanisms of haliranium ion π-ligand exchange reactions with cyclic alkenes in the gas phase. *Phys. Chem. Chem. Phys.* **2021**, *23* (45), 25572-25589.

(35) Speranza, M. Kinetics and mechanisms in gas-phase ion chemistry by radiolytic methods. *Mass Spectrom. Rev.* **1992**, *11* (2), 73-117.

(36) DePuy, C. H. Understanding Organic Gas-Phase Anion Molecule Reactions. *J. Org. Chem.* **2002**, *67* (8), 2393-2401.

(37) For other examples on the use of Hammett plots to study gas phase organic and organometallic ions using MS based methods, please refer to references 26 and 38-40.

(38) Lioe, H.; O'Hair, R. A. J. Neighbouring group processes in the deamination of protonated phenylalanine derivatives. *Org. Biomol. Chem.* **2005**, *3* (20), 3618-3628.

(39) Gray, A.; Tsybizova, A.; Roithova, J. Carboxylate-assisted C–H activation of phenylpyridines with copper, palladium and ruthenium: a mass spectrometry and DFT study. *Chem. Sci.* **2015**, *6* (10), 5544-5553.

(40) Vikse, K. L.; Henderson, M. A.; Oliver, A. G.; McIndoe, J. S. Direct observation of key intermediates by negative-ion electrospray ionisation mass spectrometry in palladium-catalysed cross-coupling. *Chem. Commun.* **2010**, *46* (39), 7412-7414.

(41) Zavras, A.; Ghari, H.; Ariafard, A.; Canty, A. J.; O'Hair, R. A. J. Gas-Phase Ion–Molecule Reactions of Copper Hydride Anions $[CuH_2]^-$ and $[Cu_2H_3]^-$. *Inorg. Chem.* **2017**, *56* (5), 2387-2399.

(42) The calculated relative enthalpy changes used to justify the observed shift in reactivity partitioning are near the error inherent in the DFT calculations at this level of theory (around 5-8 kJ mol^{-1} based on the M06-2X functional with similar sized basis sets as noted in references 61, 64, and 67). Nevertheless, the relative errors are likely smaller given the comparisons being made here and most importantly are supported by experimental observations in this study.

(43) A reviewer queried whether the rapidly formed addition product formed is covalently bonded or instead an ion-molecule complex. We would argue the former as weakly bound ion-molecule complexes exhibit peak fronting in the mass spectrum due to fragmentation of the fragile ions upon ejection from the ion trap and we did not observe this phenomenon in our experiments (see reference 44 for further information on peak fronting). Further, our calculations on addition of *cis*-cyclooctene to the selenonium ion also support a practically barrierless pathway (Figure S22), which is consistent with the rapid addition observed.

(44) Murphy Iii, J. P.; Yost, R. A. Origin of mass shifts in the quadrupole ion trap: dissociation of fragile ions observed with a hybrid ion trap/mass filter instrument. *Rapid Commun. Mass Spectrom.* **2000**, *14* (4), 270-273.

(45) Brydon, S. C.; White, J. M.; O'Hair, R. A. J. Effects of the β-Heteroatom and Leaving Group on Neighbouring Group Participation in the Gas Phase: A Density Functional Theory Study. *J. Phys. Org. Chem.* **2022**, *35* (12), e4426.

(46) Bohme, D. K. Proton transport in the catalyzed gas-phase isomerization of protonated molecules. *Int. J. Mass Spectrom. Ion Processes* **1992**, *115* (2), 95-110.

(47) Glukhovtsev, M. N.; Pross, b. A.; Radom, L. Gas-Phase Identity S_N2 Reactions of Halide Anions with Methyl Halides: A High-Level Computational Study. *J. Am. Chem. Soc.* **1995**, *117* (7), 2024-2032.

(48) Shorter, J. The separation of polar, steric, and resonance effects in organic reactions by the use of linear free energy relationships. *Q. Rev. Chem. Soc.* **1970**, *24* (3), 433-453.

(49) Reid, G. E.; Simpson, R. J.; O'Hair, R. A. J. Leaving group and gas phase neighboring group effects in the side chain losses from protonated serine and its derivatives. *J. Am. Soc. Mass. Spectrom.* **2000**, *11* (12), 1047-1060.

(50) Pekar Second, T.; Blethrow, J. D.; Schwartz, J. C.; Merrihew, G. E.; MacCoss, M. J.; Swaney, D. L.; Russell, J. D.; Coon, J. J.; Zabrouskov, V. Dual-Pressure Linear Ion Trap Mass Spectrometer Improving the Analysis of Complex Protein Mixtures. *Anal. Chem.* **2009**, *81* (18), 7757-7765.

(51) Makarov, A.; Denisov, E.; Kholomeev, A.; Balschun, W.; Lange, O.; Strupat, K.; Horning, S. Performance Evaluation of a Hybrid Linear Ion Trap/Orbitrap Mass Spectrometer. *Anal. Chem.* **2006**, *78* (7), 2113-2120.

(52) Olsen, J. V.; Schwartz, J. C.; Griep-Raming, J.; Nielsen, M. L.; Damoc, E.; Denisov, E.; Lange, O.; Remes, P.; Taylor, D.; Splendore, M.; Wouters, E. R.; Senko, M.; Makarov, A.; Mann, M.; Horning, S. A Dual Pressure Linear Ion Trap Orbitrap Instrument with Very High Sequencing Speed*. *Mol. Cell. Proteomics* **2009**, *8* (12), 2759-2769.

(53) Donald, W. A.; Khairallah, G. N.; O'Hair, R. A. J. The Effective Temperature of Ions Stored in a Linear Quadrupole Ion Trap Mass Spectrometer. *J. Am. Soc. Mass. Spectrom.* **2013**, *24* (6), 811-815.

(54) Gronert, S.; DePuy, C. H.; Bierbaum, V. M. Deuterium isotope effects in gas-phase reactions of alkyl halides: distinguishing E2 and S(N)2 pathways. *J. Am. Chem. Soc.* **1991**, *113* (10), 4009-4010.

(55) Waters, T.; O'Hair, R. A. J.; Wedd, A. G. Catalytic Gas Phase Oxidation of Methanol to Formaldehyde. *J. Am. Chem. Soc.* **2003**, *125* (11), 3384-3396.

(56) Su, T.; Bowers, M. T. Theory of ion-polar molecule collisions. Comparison with experimental charge transfer reactions of rare gas ions to geometric isomers of difluorobenzene and dichloroethylene. *J. Chem. Phys.* **1973**, *58* (7), 3027-3037.

(57) Su, T.; Bowers, M. T. Ion-Polar molecule collisions: the effect of ion size on ion-polar molecule rate constants; the parameterization of the average-dipole-orientation theory. *Int. J. Mass Spectrom. Ion Phys.* **1973**, *12* (4), 347-356.

(58) Su, T.; Bowers, M. T. Ion-polar molecule collisions. Effect of molecular size on ion-polar molecule rate constants. *J. Am. Chem. Soc.* **1973**, *95* (23), 7609-7610.

(59) Lim, K. F. COLRATE. QCPE 643: Calculation of gas-kinetic collision rate coefficients. *Quantum Chem. Program Exch.* **1994**, *14* (1), 3.

(60) Frisch, M. J. T., G. W.; Schlegel, H. B.; Scuseria, G. E.; Robb, M. A.; Cheeseman, J. R.; Scalmani, G.; Barone, V.; Petersson, G. A.; Nakatsuji, H.; Li, X.; Caricato, M.; Marenich, A. V.; Bloino, J.; Janesko, B. G.; Gomperts, R.; Mennucci, B.; Hratchian, H. P.; Ortiz, J. V.; Izmaylov, A. F.; Sonnenberg, J. L.; Williams-Young, D.; Ding, F.; Lipparini, F.; Egidi, F.; Goings, J.; Peng, B.; Petrone, A.; Henderson, T.; Ranasinghe, D.; Zakrzewski, V. G.; Gao, J.; Rega, N.; Zheng, G.; Liang, W.; Hada, M.; Ehara, M.; Toyota, K.; Fukuda, R.; Hasegawa, J.; Ishida, M.; Nakajima, T.; Honda, Y.; Kitao, O.; Nakai, H.; Vreven, T.; Throssell, K.; Montgomery, J. A., Jr.; Peralta, J. E.; Ogliaro, F.; Bearpark, M. J.; Heyd, J. J.; Brothers, E. N.; Kudin, K. N.; Staroverov, V. N.; Keith, T. A.; Kobayashi, R.; Normand, J.; Raghavachari, K.; Rendell, A. P.; Burant, J. C.; Iyengar, S. S.; Tomasi, J.; Cossi, M.; Millam, J. M.; Klene, M.; Adamo, C.; Cammi, R.; Ochterski, J. W.; Martin, R. L.; Morokuma, K.; Farkas, O.; Foresman, J. B.; Fox, D. J. Gaussian 16, Revision C.01. Gaussian, Inc. Wallingford, CT: 2019.

(61) Zhao, Y.; Truhlar, D. G. The M06 suite of density functionals for main group thermochemistry, thermochemical kinetics, noncovalent interactions, excited states, and transition elements: two new functionals and systematic testing of four M06-class functionals and 12 other functionals. *Theor. Chem. Acc.* **2008**, *120* (1), 215-241.

(62) Grimme, S.; Antony, J.; Ehrlich, S.; Krieg, H. A consistent and accurate ab initio parametrization of density functional dispersion correction (DFT-D) for the 94 elements H-Pu. *J. Chem. Phys.* **2010**, *132* (15), 154104.

(63) Weigend, F.; Ahlrichs, R. Balanced basis sets of split valence, triple zeta valence and quadruple zeta valence quality for H to Rn: Design and assessment of accuracy. *Phys. Chem. Chem. Phys.* **2005**, *7* (18), 3297-3305.

(64) Mardirossian, N.; Head-Gordon, M. How Accurate Are the Minnesota Density Functionals for Noncovalent Interactions, Isomerization Energies, Thermochemistry, and Barrier Heights Involving Molecules Composed of Main-Group Elements? *J. Chem. Theory Comput.* **2016**, *12* (9), 4303-4325.

(65) Dau, P. D.; Armentrout, P. B.; Michelini, M. C.; Gibson, J. K. Activation of carbon dioxide by a terminal uranium–nitrogen bond in the gas-phase: a demonstration of the principle of microscopic reversibility. *Phys. Chem. Chem. Phys.* **2016**, *18* (10), 7334-7340.

(66) Henchman, M. Entropy-Driven Reactions: Summary of the Panel Discussion. In *Structure/Reactivity and Thermochemistry of Ions*, Ausloos, P., Lias, S. G. Eds.; Springer Netherlands, 1987; pp 381-399.

(67) Zheng, J.; Zhao, Y.; Truhlar, D. G. The DBH24/08 Database and Its Use to Assess Electronic Structure Model Chemistries for Chemical Reaction Barrier Heights. *J. Chem. Theory Comput.* **2009**, *5* (4), 808-821.

(68) Lafayette, L.; Sauter, G.; Vu, L.; Meade, B. Spartan Performance and Flexibility: An HPC-Cloud Chimera. OpenStack Summit, Barcelona. Oct 27, **2016**.

Table of Contents Graphic